European Journal of Medicinal Chemistry 81 (2014) 106–118

Contents lists available at ScienceDirect

European Journal of Medicinal Chemistry

journal homepage: http://www.elsevier.com/locate/ejmech

Original article

Tamiphosphor monoesters as effective anti-influenza agents

Chun-Lin Chen [a], Tzu-Chen Lin [a], Shi-Yun Wang [b], Jiun-Jie Shie [b], Keng-Chang Tsai [c], Yih-Shyun E. Cheng [b], Jia-Tsrong Jan [b], Chun-Jung Lin [d,**], Jim-Min Fang [a,b,*], Chi-Huey Wong [b,**]

[a] Department of Chemistry, National Taiwan University, Taipei 106, Taiwan, ROC
[b] The Genomics Research Center, Academia Sinica, Taipei 115, Taiwan, ROC
[c] National Research Institute of Chinese Medicine, Taipei 112, Taiwan, ROC
[d] School of Pharmacy, National Taiwan University, Taipei 100, Taiwan, ROC

ARTICLE INFO

Article history:
Received 31 March 2014
Received in revised form
28 April 2014
Accepted 30 April 2014
Available online 2 May 2014

Keywords:
Influenza
Virus
Neuraminidase
Inhibitor
Pharmacokinetics
Molecular modeling

InChIKey:
BQLKEXSYWRBWQK-AFMQGRBTSA-N

ABSTRACT

Oseltamivir is a potent neuraminidase inhibitor for influenza treatment. By replacing the carboxylate group in oseltamivir with phosphonate monoalkyl ester, a series of tamiphosphor derivatives were synthesized and shown to exhibit high inhibitory activities against influenza viruses. Our molecular modeling experiments revealed that influenza virus neuraminidase contains a 371-cavity near the S1-site to accommodate the alkyl substituents of tamiphosphor monoesters to render appreciable hydrophobic interactions for enhanced affinity. Furthermore, guanidino-tamiphosphor (TPG) monoesters are active to the oseltamivir-resistant mutant. TPG monohexyl ester **4e** having a more lipophilic alkyl substituent showed better cell permeability and intestinal absorption than the corresponding monoethyl ester **4c**, but both compounds showed similar bioavailability. Intranasal administration of TPG monoesters at low dose greatly improved the survival rate of mice infected with lethal dose of H1N1 influenza virus, whereas **4c** provided better protection of the infected mice than oseltamivir and other phosphonate congeners by oral administration.

1. Introduction

Influenza is a highly contagious disease that occurs in seasonal epidemics and also emerges periodically to global pandemics. Influenza viruses are negative-sense single-stranded RNA viruses of the family Orthomyxoviridae. The 8 RNA gene segments replicate at least 11 proteins [1,2]. Hemagglutinin (HA) and neuraminidase (NA) are the most significant surface glycoproteins for influenza virulence. Depending on the specific strain of influenza virus, HA selectively binds to human or avian respiratory epithelial cells. Influenza NA catalyzes the hydrolysis of the terminal sialic acid residue from the sialo-receptors of host cells to facilitate the release of progeny viruses for propagation and infectivity [3].

NA is a good drug target in view of its rather conserved active site [4–6]. Four NA inhibitors zanamivir (Relenza™) [7,8], oseltamivir (Tamiflu™ as the phosphate salt) [9,10], peramivir (Rapiacta™) [11,12] and laninamivir (Inavir™) [13,14] have been approved for use as anti-influenza drugs. The phosphate salt of oseltamivir (OS, **1b**), is currently the most popular oral medication for influenza therapy. Oseltamivir is converted by endogenous esterase to oseltamivir carboxylate (OC, **1a**) which is the active component for NA inhibition [3,15,16]. The carboxylic acid in OC provides multiple electrostatic interactions with the three arginine residues (R118, R292 and R371) in NA [4–6]. However, oseltamivir-resistant viruses have occurred over the years. New anti-influenza drugs that can also inhibit oseltamivir-resistant strains, such as

Abbreviations: AUC, area under the concentration-versus-time curve; CC_{50}, 50% cytotoxicity concentration; CL, clearance; CPE, cytopathic effect; *D*, distribution coefficient; DMEM, Dulbecco's modified Eagle medium; EC_{50}, half maximal effective concentration; EDTA, ethylenediaminetetraacetic acid; *F* (%), oral bioavailability (fraction absorbed); GOC, guanidino-oseltamivir carboxylic acid; GOS, guanidino-oseltamivir; HBTU, *o*-benzotriazol-1-yl-*N*,*N*,*N*′,*N*′-tetramethyluronium hexafluorophosphate; IC_{50}, half maximal inhibitory concentration; i.p., intraperitoneal; i.v., intravenous; LD_{50}, median lethal dose; MDCK, Madin–Darby canine kidney; MUNANA, 2-(4-methylumbelliferyl)-α-D-*N*-acetylneuraminic acid; NA, neuraminidase; OC, oseltamivir carboxylic acid; OS, oseltamivir; *P*, partition coefficient; $TCID_{50}$, 50% cell culture infectious dose; TP, tamiphosphor; TPG, guanidino-tamiphosphor.

* Corresponding author. Department of Chemistry, National Taiwan University, Taipei, 106, Taiwan, ROC.
** Corresponding authors.
E-mail addresses: clementumich@ntu.edu.tw (C.-J. Lin), jmfang@ntu.edu.tw (J.-M. Fang), chwong@gate.sinica.edu.tw (C.-H. Wong).

http://dx.doi.org/10.1016/j.ejmech.2014.04.082
0223-5234/

the clinically relevant H275Y mutant, are in urgent need for our fight against the threat of pandemic influenza. Compound **2a** (GOC) shows higher inhibitory activity than OC by replacing the C-5 amino group with a more basic guanidino group, which is considered to exert stronger interactions with the acidic residues (E119, D151, and E227) in the active site of influenza NA [9]. However, compound **2a** and its ethyl ester (**2b**, GOS) have not been developed for therapeutic use.

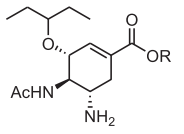

1a (OC), R = H
1b (OS), R = C_2H_5

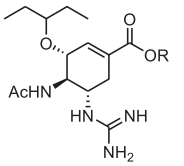

2a (GOC), R = H
2b (GOS), R = C_2H_5

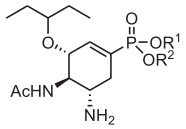

3a (TP), $R^1 = R^2 = H$
3b, $R^1 = R^2 = CH_2CH_3$
3c, $R^1 = H$, $R^2 = CH_2CH_3$
3d, $R^1 = H$, $R^2 = (CH_2)_3CH_3$
3e, $R^1 = H$, $R^2 = (CH_2)_5CH_3$
3f, $R^1 = H$, $R^2 = (CH_2)_3Ph$
3g, $R^1 = H$, $R^2 = (CH_2)_3$-(3-indole)

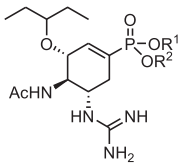

4a (TPG), $R^1 = R^2 = H$
4b, $R^1 = R^2 = CH_2CH_3$
4c, $R^1 = H$, $R^2 = CH_2CH_3$
4d, $R^1 = H$, $R^2 = (CH_2)_3CH_3$
4e, $R^1 = H$, $R^2 = (CH_2)_5CH_3$
4f, $R^1 = H$, $R^2 = (CH_2)_3Ph$

Formation of phosphonate–guanidinium complex is thermodynamically favored [17]. Tamiphosphor (TP, **3a**), a phosphonate congener of OC, is thus designed to have strong electrostatic interactions with the three arginine residues (R118, R292 and R371) in the active site of NA [18,19]. The phosphonate ion in **3a** is also topologically complementary to bind with the three arginine residues. Compound **3a** has high NA inhibitory activities to suppress the replication of human and avian influenza viruses. Our previous study [19] indicates that phosphonate monoethyl ester **3c** is also very active to protect human 293T and canine MDCK cells from infection by influenza viruses because **3c** still contains a negative charge at the phosphonate group to render the necessary electrostatic interactions with the three arginine residues in NA. Monoester **3c** is a drug, instead of a prodrug, because it does not metabolize to the free phosphonic acid **3a** in animal experiments [19]. In another approach, Streicher and coworkers have demonstrated that the phospha-oseltamivir monoesters carrying various functional groups can be of versatile uses [20–23]. For example, the phospha-oseltamivir monoesters equipped with aglycone mimetics or linked to gold nanoparticles are good for treatment and detection of influenza viruses.

We have also prepared guanidino-tamiphosphor (TPG, **4a**) and its monoethyl ester **4c** to show that they possess high inhibitory activities against the oseltamivir-resistant mutant of influenza virus. In contrast, phosphonate diethyl esters **3b** and **4b** are inactive to influenza viruses. The phosphonate compounds **3a**, **3c**, **4a** and **4c** have similar pharmacokinetic properties in mice, rats and dogs. TPG monoester **4c** in saline solution shows better oral bioavailability ($F = 12\%$) than TPG **4a** ($F = 7\%$) in mice [19]. We therefore aim to investigate whether the bioavailability and pharmacokinetic properties can be further improved in the TP and TPG monoalkyl esters bearing more lipophilic alkyl groups, such as **3d**–**3g** and **4d**–**4f**.

In another aspect, a flexible 150-loop adjacent to the S2 active site is found from the X-ray crystallographic studies of the apo and inhibitor-bound structures of NAs [6,24]. The A-type influenza virus NAs are divided into two categories: group-1 including N1, N4, N5 and N8 subtypes, and group-2 comprising N2, N3, N6, N7 and N9 subtypes. It is proposed that the 150-loop of group-2 NA always exists in the closed form, whereas that of group-1 NA would change from the open conformation to the closed form on binding with substrate or inhibitor. In contrast, molecular dynamics simulations suggest that both group-1 and group-2 NAs are able to adopt an open 150-cavity within their solution-phase structural ensemble [25]. Molecular dynamics simulations of influenza NAs further indicate the existence of a 430-loop comprising the residues R430–T439 adjacent to the S1 active site [26,27]. The conformational change of 150-loop may be coupled with motion of the neighboring 430-loop to form a much larger binding pocket than that shown in the static crystal structures. In this study, we carried out molecular modeling experiments to reveal that influenza virus also contains a hydrophobic 371-cavity near the NA active site that may provide additional interactions with the alkyl groups in our designed inhibitors of phosphonate monoesters.

2. Results and discussion

2.1. Molecular modeling

The structure-based design of NA inhibitors has been a successful strategy in discovery of anti-influenza drugs [4]. The phosphonate group has been used as a bioisostere of carboxylate in drug design [29–31]. In comparison with carboxylate ion, a phosphonate ion exhibits stronger electrostatic interactions with guanidinium ion [17]. Formation of phosphonate–guanidinium complex is thermodynamically favored [17]. Consistent with this rationale, compound **3a** containing a phosphonic acid binds strongly with the three arginine residues in the NA active site, thus showed higher inhibitory activity than the corresponding carboxylate **1a** against various human and avian influenza viruses, including A/H1N1 (wild-type and H275Y mutant), A/H5N1, A/H3N2 and type B viruses [19]. Using the known N1 crystal structure (PDB code: 2HU4) [6], our molecular docking experiments indicated that the phosphonate group of **3a** formed 8-pair hydrogen bonds with three arginine residues (Fig. 1A), greater than the carboxyl group of **1a** (6 pairs of hydrogen bonds). The monoalkyl phosphonate ion, e.g. **3f**, exhibited 7 pairs of hydrogen bonds with the three arginine residues in the S1 site of NA (Fig. 1B), in addition to the appreciable interactions of the C_3-pentoxy, C_4-acetamido and C_5-amino groups in the S2–S5 sites [5]. Our molecular modeling revealed that the 3-phenylpropyl moiety in **3f** also exhibited considerable interactions with I427, P431 and K432 residues in the 430-loop. This result is in agreement with the prediction by ensemble-based virtual screening [32], which shows that the 430-cavity of NA favors to accept aromatic rings and hydrophobic substituents.

Moreover, we found a hydrophobic cleft, namely 371-cavity (Fig. 1D), was enclosed by the R371, P431, I427, K432 and W403 residues located between the 430- and 371-loops near the S1 site. The 3-phenylpropyl substituent of **3f** extended to the 371-cavity, so that the phenyl group was disposed in a manner to exert a significant π–cation interaction with R371, and a T-shape interaction with the indole ring of the W403 residue in an edge-to-face configuration [33]. In a similar fashion, the (indol-3-yl)propyl substituent of **3g** was located in the region of 430- and 371-loops to attain additional hydrophobic, π–π and π–cation interactions (Fig. 1C). Thus, phosphonate monoesters **3f** and **3g** were predicted to possess high affinity to influenza virus NAs.

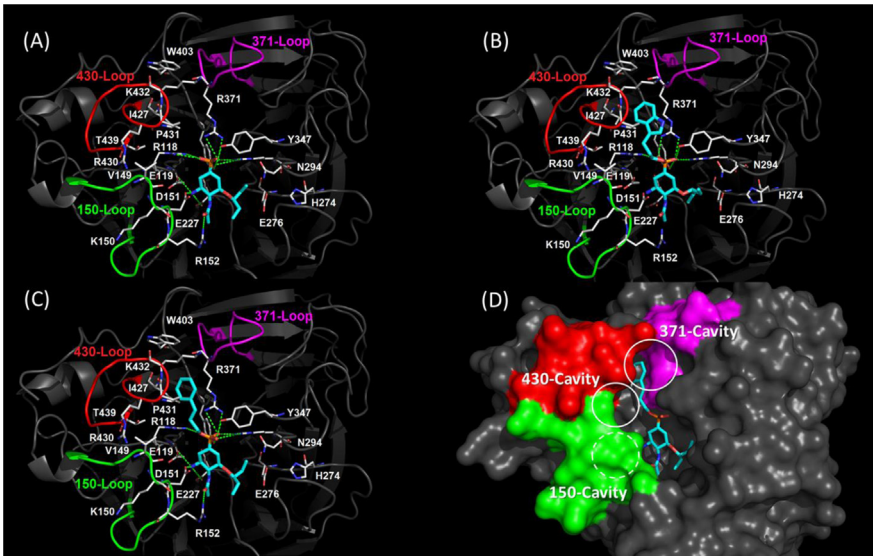

Fig. 1. Molecular models of tamiphosphor **3a** (A) and phosphonate monoalkyl esters **3f** (B) and **3g** (C) in the active site of influenza virus neuraminidase (N1 subtype, PDB code: 2HU4). The phenylpropyl group of **3f** embedded in a 371-cavity near S1 site is shown (D). The phosphonic acid moiety of **3a** exhibits extensive hydrogen bonding interactions (8 pairs ligand–NA H-bonds) with three arginine residues (R118, R292 and R371) in the NA active site. In the **3f**–NA or **3g**–NA complex, there are 7 pairs H-bonds formed by the phosphonate monoester group with R118, R292 and R371. However, the phenylpropyl substituent in **3f** and (indol-3-yl)propyl substituent in **3g** extend to the 371-cavity to gain appreciable hydrophobic, π–π and π–cation interactions.

2.2. Chemical synthesis

We have previously synthesized phosphonic acids **3a** and **4a** using D-xylose as an inexpensive starting material via an intramolecular Horner–Wadsworth–Emmons reaction with tetraethyl methylenediphosphonate ($H_2C[PO(OEt)_2]_2$) to construct the desired cyclohexenephosphonate scaffold [18]. In another approach, Streicher [20], Gunasekera [28] and our research teams [29] have provided an effective synthesis of oseltamivir phosphonate congeners using a palladium-catalyzed phosphonylation of 1-halocyclohexene as the key reaction. We applied this method to synthesize a series of phosphonate monoesters **3c**–**3g** and **4c**–**4f** as shown in Scheme 1. The *N*-Boc protected oseltamivir (**5**) [29] was hydrolyzed to give the corresponding carboxylic acid **6** [28], which was further converted to Barton ester [30,31] for the subsequent photolysis, giving the iodocyclohexene derivative **7** in the presence of CF_3CH_2I [20,28]. On the other hand, the phosphite reagents **8c**–**8g** were readily prepared from phosphorus trichloride with 2 equiv of appropriate alcohols, including ethanol, butanol, hexanol, 3-phenylpropanol and 3-(indol-3-yl)propanol. Thus, the iodo compound **7** was subject to a Pd-catalyzed phosphonylation with dialkyl phosphites **8c**–**8g** to afford the phosphonate compounds **9c**–**9g**. The Boc protecting group in **9c**–**9g** was removed by trifluoroacetic acid (TFA), and the phosphonate dialkyl esters were treated with aqueous KOH to cleave one alkyl group, giving the desired phosphonate monoalkyl esters **3c**–**3g**. Alternatively, the amine intermediate was reacted with *N*,*N*′-bis-(*tert*-butoxycarbonyl)-*S*-methylisothiourea in the presence of $HgCl_2$ and Et_3N to give **10c**–**10f**, which were converted to TPG monoalkyl esters **4c**–**4f** by sequential treatments with TFA and $KOH_{(aq)}$.

2.3. Lipophilicity of phosphonate monoesters

In the design of an orally available drug, lipophilicity is an important pharmacokinetic factor that must be considered. With appropriate lipophilicity, drugs can diffuse through cell membrane and thus having better bioavailability. The partition coefficient (*P*) is a measure of lipophilicity for nonionic compound between octanol and water, and oral drugs are often found to have log *P* values between −1 and 5 [34]. In lieu of log *P*, the distribution coefficient (log *D*) is generally used to represent the partition of an ionic compound between octanol and PBS buffer under specific pH value. Despite having double negative charges on the phosphonate group, **3a** (log $D = -1.04$) appeared to be less hydrophilic than OC (log

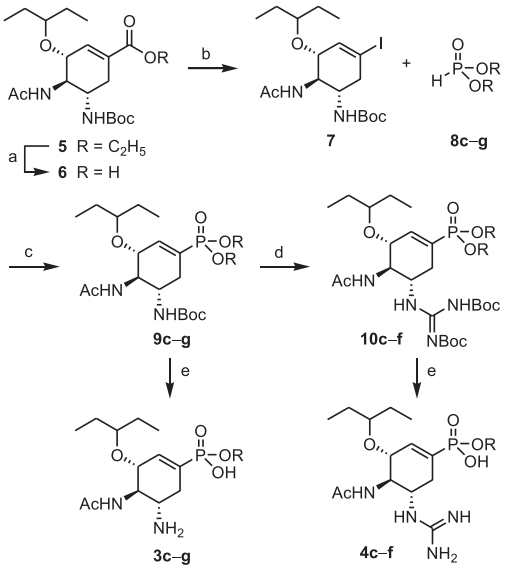

Scheme 1. Synthesis of tamiphosphor and guanidino-tamiphosphor monoesters. Reagents and conditions: (a) 1 M $KOH_{(aq)}$, MeOH, 25 °C, 2 h; 90%. (b) 3-hydroxy-4-methyl-2(3*H*)-thiazolethione, HBTU, Et_3N, CH_2Cl_2, 25 °C, 2 h; then CF_3CH_2I, CH_2Cl_2, hν, 30 min; 54% overall yield. (c) $Pd(PPh_3)_4$, toluene, Et_3N, 90 °C, 2–12 h; 64–86%. (d) CF_3COOH, CH_2Cl_2, 25 °C, 1 h; then *N*,*N*′-bis-(*tert*-butoxycarbonyl)-*S*-methyl-isothiourea, $HgCl_2$, Et_3N, CH_2Cl_2, 25 °C, 2–3 h; 60–75%. (e) CF_3COOH, CH_2Cl_2, 25 °C, 2 h; $KOH_{(aq)}$, 1,4-dioxane, 25–40 °C, 24–120 h; 43–68%. HBTU = *o*-Benzotriazol-1-yl-*N*,*N*,*N*′,*N*′-tetramethyluronium hexafluorophosphate.

$D = -1.69$) that carries a single negative charge [19]. Table 1 shows the calculated and measured values of log D for a series of phosphonate derivatives. All the phosphonate monoesters had higher log D values than their parental acids **3a** and **4a** (log $D = -0.98$). The lipophilicity of phosphonate monoesters increased as the aliphatic chain elongated. The log D value increased about 1 unit when hexyl monoester compound **3e** (log $D = 0.30$) is compared to ethyl monoester **3c** (log $D = -0.75$) [19]. Monoesters **3f** and **4f** having 3-phenylpropyl substituent showed the lipophilicity similar to the monohexyl esters **3e** and **4e**. Interestingly, we also found that guanidino-phosphonates **4c**–**4f** were more lipophilic than their corresponding amino compounds **3c**–**3f**. This result was in agreement with the trend of calculation (*c* log *D*). The improved lipophilic property of guanidino compounds might be related to their zwitterionic structures [35,36], in which the C-5 guanidinium could form ion-pair with the phosphonate group more favorably (in comparison, guanidinium p$K_a \approx 14$ versus aminium p$K_a \approx 10$) [17,37,38]. Without having zwitterionic structure, phosphonate diethyl ester **4b** (log $D = -0.10$) bearing a more basic guanidine substituent was less lipophilic than **3b** (log $D = 0.22$) having an amine substituent at the C-5 position [19].

2.4. Neuraminidase inhibition and anti-influenza activity

The NA inhibitory activity was measured using a fluorogenic substrate 2-(4-methylumbelliferyl)-α-D-*N*-acetylneuraminic acid (MUNANA). The anti-influenza activities were measured by protection of Madin–Darby canine kidney (MDCK) cells from the viral infection. OS (**1b**) as an ester is inactive to NA while its carboxylic acid **1a** is a nanomolar NA inhibitor of influenza virus. The phosphonic acids **3a** and **4a** also effectively inhibited the H1N1 virus NA with $IC_{50} \approx 2$ nM [19]. Table 2 shows the NA inhibition (IC_{50}) and anti-influenza activities (EC_{50}) of TP and TPG monoalkyl esters against wild-type H1N1 virus (A/WSN/1933) and OS-resistant H275Y mutant. Unlike OS, the phosphonate monoalkyl esters **3c**–**g** and **4c**–**f** all showed high NA inhibitory activities against wild-type H1N1 virus ($IC_{50} = 1.6$–6.9 nM). This result is in agreement with our molecular docking experiments. Phosphonate monoester has a negative charge to render sufficient electrostatic interactions with R118, R292 and R371, and the alkyl substituent may also provide appreciable hydrophobic interactions to increase the affinity with NA. Though TP monoesters were inactive to H275Y mutant, TPG monoesters **4c**–**4f** still showed strong inhibition to the OS-resistant H275Y virus with $IC_{50} < 90$ nM and $EC_{50} < 1$ μM. The cell-based assays indicated that the anti-influenza agents **3c**–**3g** and **4c**–**4f** were nontoxic to human 293T and canine MDCK cells at the highest testing concentrations (>10 μM).

Table 1
Distribution coefficients of tamiphosphor monoalkyl esters.

Compound	*c* log *P*[a]	*c* log *D*[b]	log *D*[c,d]
3c	−0.14 (−0.40)	−1.53	−0.75 ± 0.10
3d	0.93 (0.51)	−0.61	−0.29 ± 0.04
3e	1.99 (1.35)	0.23	0.30 ± 0.06
3f	1.95 (1.67)	0.54	0.28 ± 0.02
4c	−0.81 (−0.34)	−1.27	−0.37 ± 0.02
4d	0.26 (0.57)	−0.36	−0.16 ± 0.06
4e	1.32 (1.41)	0.48	0.63 ± 0.08
4f	1.29 (1.73)	0.80	0.66 ± 0.04

[a] Calculated values using Advanced Chemistry Development (ACD/Laboratories) Software V12.01. Data in parenthesis were calculated using MarvinSketch (http://www.chemaxon.com/marvin/sketch/index.html).
[b] Calculated values using MarvinSketch.
[c] Octanol–water partition coefficient determined at pH 7.4 from five repeated experiments.
[d] Log *D* value at pH 7.4 (adapted from literature [39]).

Table 2
Inhibitory activities of tamiphosphor monoalkyl esters against wild-type H1N1 and oseltamivir-resistant influenza viruses.[a]

Compound[b]	Wt (WSN)[a]		H275Y[a]	
	IC_{50} (nM)[c]	EC_{50} (nM)[d]	IC_{50} (nM)[c]	EC_{50} (nM)[d]
3c[e]	3.0 ± 2.0	47 ± 4	1679 ± 43	490 ± 470
3d	6.9 ± 2.0	58.6 ± 6.2	1443 ± 14	9154 ± 32
3e	2.2 ± 0.5	18.3 ± 0.4	1719 ± 56	>10,000[e]
3f	1.8 ± 0.7	13.1 ± 6.9	1283 ± 12	>10,000[e]
3g	1.7 ± 0.1	13.1 ± 9.5	ND[f]	ND[f]
4c[e]	1.1 ± 0.1	180 ± 14	25.1 ± 6.6	900 ± 200
4d	6.7 ± 3.1	7.6 ± 3.5	10.9 ± 1.3	97 ± 18
4e	4.1 ± 0.8	9.3 ± 8.7	89.2 ± 9.5	262 ± 11
4f	3.2 ± 0.8	3.3 ± 2.1	24.6 ± 1.3	224 ± 16

[a] Influenza viruses A/WSN/1933 (H1N1) and the H274Y mutant were used as bioassay materials for neuraminidase inhibition and anti-influenza assays.
[b] The test compounds **3c**–**3g** and **4c**–**4f** were nontoxic to human 293T and canine MDCK cells at the highest testing concentrations (>10 μM).
[c] A fluorescent substrate, 2-(4-methylumbelliferyl)-α-D-*N*-acetylneuraminic acid (MUNANA), was used to determine the IC_{50} values that are compound concentrations causing 50% inhibition of different influenza neuraminidase enzymes. Data are shown as mean ± SD of three experiments.
[d] The anti-influenza activities against different influenza strains were measured as EC_{50} values that are the compound concentrations for 50% protection of the cytopathic effects due to the infection by different influenza strains. Data are shown as mean ± SD of three experiments.
[e] The data are adapted from literature [19].
[f] ND: Not determined.

2.5. Cellular uptake

The MDCK cellular uptake study (Fig. 2) showed that phosphonate monoester **4e** (R = hexyl) was much more permeable than **4c** (R = ethyl) and **4f** (*R* = 3-phenylpropyl). In the first 10 min, the cell permeability of **4e** increased more than 10 fold than **4c** and **4f**. Furthermore, the concentration of **4e** reached 13,500 ng/mg protein in 120 min, whereas **4c** and **4f** were still at the concentrations lower than 2000 ng/mg protein.

2.6. Intestinal permeability

In addition to cellular uptake in renal epithelial MDCK cells, intestinal permeability of compounds **4c** and **4e** were further examined in Caco-2 cells, a model resembling human intestinal epithelial cells. The apical-to-basolateral flux (i.e., absorption) of compound **4c** was comparable to its flux in basolateral-to-apical direction (i.e., secretion), suggesting the absorption of compound

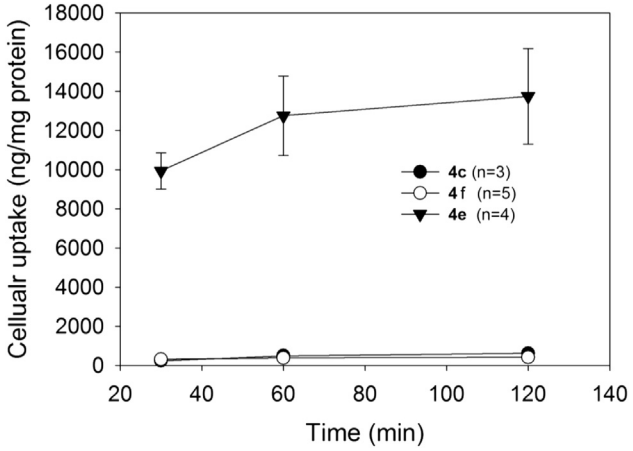

Fig. 2. MDCK cell uptake of phosphonate monoesters **4c** (R = ethyl), **4e** (R = hexyl) and **4f** (*R* = 3-phenylpropyl).

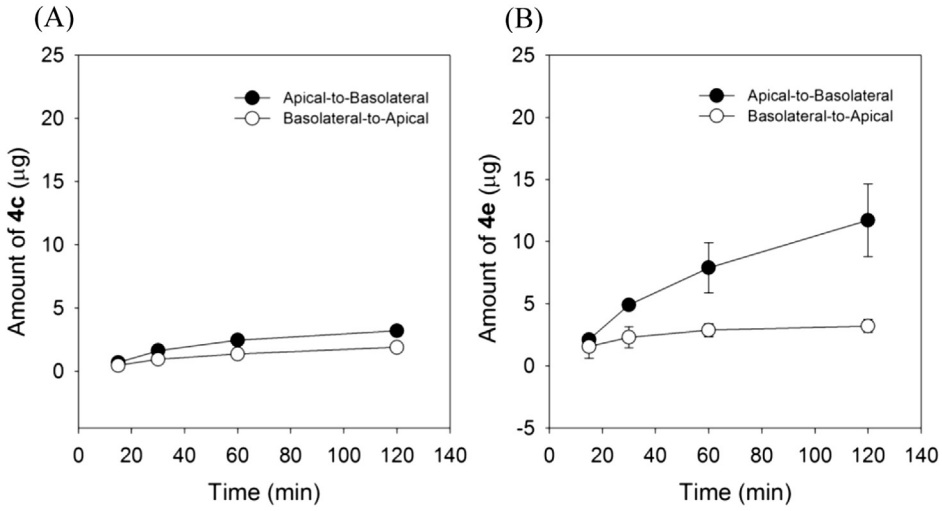

Fig. 3. Intestinal permeability of phosphonate monoesters **4c** (R = ethyl) and **4e** (R = hexyl) in Caco-2 cells.

4c is limited (Fig. 3A). In contrast, compound **4e** show significantly higher flux in the direction of apical-to-basolateral, showing its higher intestinal absorption (Fig. 3B).

2.7. Bioavailability

The pharmacokinetic parameters for compounds **4c** and **4e** in male mice are listed in Table 3. The half-life of **4e** was 0.36 h after intravenous (i.v.) administration, and 1.17 h after oral administration. In comparison with **4c** had half-lives of 0.71 and 2.57 h for i.v. and oral administration. Compound **4e** had shorter half-lives than **4c**, presumably because **4e** was a more lipophilic compound susceptible to clearance by metabolism in mice [40]. Indeed, **4e** had 2–3 fold clearance rates than **4c** in i.v. and oral administrations. The absolute oral bioavailability (*F* value) of compound **4e** was 12.6% in mice, similar to **4c** (12.1%) but better than their parental phosphonic acid **4a** (7%) [19]. Even though the hexyl monoester **4e** exhibited higher cellular uptake and permeability in MDCK and Caco-2 cells than the ethyl ester **4c**, no better bioavailability of **4e** in mice was obtained presumably due to the counteract of metabolism.

2.8. Mice protection experiments against A/WSN/33 (H1N1) virus

In one experiment, 1.2 μmol/kg/day of test compound, a dose equivalent to that of zanamivir for human therapy, was intranasally administered to mice twice-daily on days 1–4, and day 0 before infection with lethal doses (10 LD_{50}) of H1N1 influenza virus (A/WSN/1933). All mice survived at day 14 (Fig. 4A). At low dosage of 0.12 μmol/kg/day, zanamivir only provided partial protection, and all mice died at day 9. In comparison, TPG monoesters **4c**, **4e** and **4f** were superior to zanamivir in improving the survival rate of infected mice (Fig. 4B). By oral administration of test compound at a dose of 2.6 μmol/kg/day (Fig. 4C), compound **4c** (R = ethyl) exhibited much better protection of the virus infected mice than oseltamivir, **4e** and **4f**. This study indicated that monoester **4e** (R = hexyl) only exhibited a marginal mice protection effect by oral administration even it showed low EC_{50} value in the cell-based assay and similar bioavailability to **4c**.

3. Conclusion

In order to develop effective anti-influenza drugs, we have prepared a series of oseltamivir phosphonate congeners, especially focusing on the phosphonate monoesters bearing hydrophobic alkyl substituents. Using *N*-Boc protected oseltamivir carboxylic acid as a starting material, the halodecarboxylation reaction was carried out via photolysis of the Barton ester derivative in the presence of CF_3CH_2I. The Pd-catalyzed phosphonylation of the iodocyclohexene derivative **7** with dialkyl phosphites afforded the corresponding phosphonates, which were then elaborated to the desired tamiphosphor and guanidino-tamiphosphor monoesters (Scheme 1). The lipophilicity of phosphonate monoesters increased as the aliphatic chain elongated, and the guanidino-phosphonates (**4c**–**4f**) were more lipophilic than their corresponding amino compounds (**3c**–**3f**). The phosphonate monoesters showed potent NA inhibitory activities with IC_{50} values in low nanomolar range against influenza viruses. Our molecular modeling experiments

Table 3
Pharmacokinetic parameters of compounds **4c** and **4e** after single intravenous bolus or oral administration to male mice.

PK parameter (unit)	**4c**[a]		4e	
	IV, 0.25 mg/kg ($N = 6$)	Oral, 10 mg/kg ($N = 6$)	IV, 0.25 mg/kg ($N = 5$)	Oral, 10 mg/kg ($N = 3$)
k (1/h)	1.37	0.36	1.92	0.60
$AUC_{0\rightarrow t}$ (h*ng/mL)	529	2575	169[b]	361[c]
$AUC_{0\rightarrow\infty}$ (h*ng/mL)	541	2629	173	867
$T_{1/2}$ (h)	0.71	2.57	0.36	1.07
CL/F (L/h/kg)	0.47	4.75	1.45	11.05
F (%)	100	12.1	100	12.6
C_{max} (ng/mL)	–	935	–	261
T_{max} (h)	–	1.39	–	1.00

[a] The pharmacokinetic parameters of compound **4c** are the mean values adapted from literature [19].
[b] $t = 2$.
[c] $t = 12$.

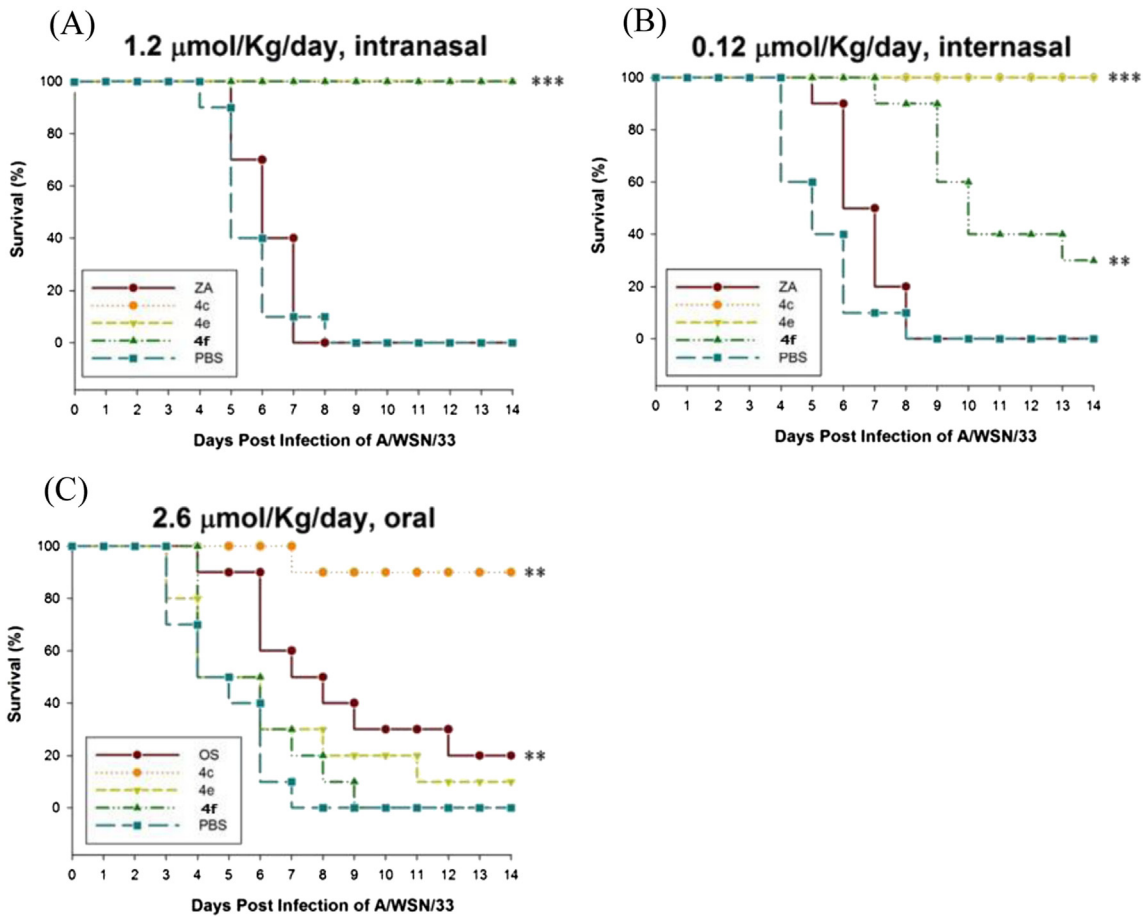

Fig. 4. Percentage of survival of mice by intranasal inoculation (A and B) or oral gavage (C) with test compounds at the indicated dosages (1.2, 0.12 and 2.6 μmol/kg/day). Mice were administered twice per day. Four hours after the first dose of test compound, mice were challenged with 10 LD_{50} of A/WSN/33 (H1N1) influenza virus. The number of mice at day 0 (10 mice per group) were defined as 100%, respectively. ***$P < 0.0001$. **$P < 0.001$.

reveal that phosphonate monoalkyl ester contains a negative charge on the phosphonate moiety to render sufficient electrostatic interactions with the three arginine residues (R118, R292 and R371) in the NA active site, and the alkyl substituent is located in the 371-cavity near the S1-site to attain extra hydrophobic interactions the enhanced affinity with NA. The cell-based assays showed that tamiphosphor, guanidino-tamiphosphor and their monoesters all exhibited potent anti-influenza activities. Guanidino-tamiphosphor monoesters were active to oseltamivir-resistant H275Y mutant with $EC_{50} < 1$ μM. Even though the phosphonate monohexyl ester **4e** has much better cell permeability and intestinal absorption than the monoethyl ester **4c**, both compounds have similar absolute bioavailability ($F \approx 12.5\%$) because **4e** also has higher metabolism rate. Intranasal administration of TPG monoesters (**4c**, **4e** or **4f**) at low dose (e.g. one tenth of zanamivir-equivalent dose) greatly improved the survival rate of mice infected with lethal dose of H1N1 influenza virus. Nevertheless, compound **4c** is still the choice for oral administration to provide effective protection of the virus infected mice (Fig. 4C).

4. Experimental section

4.1. General

All the reagents were commercially available and used without further purification unless indicated otherwise. All solvents were anhydrous grade unless indicated otherwise. All non-aqueous reactions were carried out in oven-dried glassware under a slight positive pressure of argon unless otherwise noted. Reactions were magnetically stirred and monitored by thin-layer chromatography on silica gel. Flash chromatography was performed on silica gel (60–200 μm particle size) and LiChroprep RP-18 (40–63 μm particle size). The pH values were measured with Mettler-Toledo MP-120 pH meter. Melting points were recorded on Yanaco melting point apparatus and are not corrected. Optical rotations were recorded on digital polarimeter of Japan JASCO Co. DIP-1000; $[\alpha]_D$ values are given in units of 10^{-1} deg cm^2 g^{-1}. NMR spectra were recorded on Bruker Avance-400 (400 MHz), Bruker400 AVIII (400 MHz) and Varian Unity Plus-400 (400 MHz) spectrometer. Chemical shifts are given in δ values relative to tetramethylsilane (TMS); coupling constants J are given in Hz. Internal standards were δ_H 7.24/δ_C 77.0 (central line of t) for $CHCl_3/CDCl_3$, δ_H 4.80 for H_2O/D_2O, δ_H 3.31/δ_C 48.2 for CD_3OD, and H_3PO_4 in D_2O ($\delta_P = 0$) for ^{31}P NMR spectra. The splitting patterns are reported as s (singlet), d (doublet), t (triplet), q (quartet), m (multiplet), br (broad) and dd (double of doublets). IR spectra were recorded on a Nicolet Magna 500-II. High resolution ESI mass spectra were recorded on a Bruck Daltonics BioTOF III high-resolution mass spectrometer. High-performance liquid chromatography (HPLC) was performed on Agilent 1100 series equipped with a degasser, Quat pump, and UV detector.

4.2. Viruses

Influenza A/WSN/1933 (H1N1) virus was obtained from Dr. Shin-Ru Shih at Chang Gung University in Taiwan. WSN 275Y was

selected with tamiflu from influenza A/WSN/1933 (H1N1) in our laboratory. All viruses were cultured in the allantoic cavities of 10-day-old embryonated chicken eggs for 72 h, and purified by sucrose gradient centrifugation. Madin–Darby canine kidney (MDCK) cells were obtained from American Type Culture Collection (Manassas, Va), and were grown in DMEM (Dulbecco's modified Eagle medium, GibcoBRL) containing 10% fetal bovine serum (GibcoBRL) and penicillin-streptomycin (GibcoBRL) at 37 °C under 5% CO_2.

4.3. Computer modeling

The model of a specific compound in complex with the NA was constructed through docking this compound to the crystallographic structure of N1 neuraminidase (PDB code: 2HU4) [6]. The 3D structure of compound (**3a**, **3f** or **3g**) was built by modifying the 3D structure of oseltamivir acid (**1a**, from 2HU4) with SYBYL 8.0 program (Tripos Associates, St. Louis, MO). GOLD 4.0.115 was used to dock the compound onto the protein with flexible docking option turned on [41,42]. Kollmann-all atom charges [43] were assigned to the protein atoms, and Gasteiger–Hückel charges [44] were assigned to ligand atoms using the SYBYL 8.0 program. Initial 1000 independent genetic algorithm cycles of computation were carried out with ligand torsion angles varying between −180 and 180°. The search efficiency was set at 200% to ensure the most exhaustive search for the docking conformational space. All other parameters were kept the same as the default settings. The docking processes were distributed to a 40-processor Linux cluster with Intel(R) Xeon(TM) CPU 3.00 GHz CPUs. The resultant ligand–protein complex structures were ranked with the GOLDSCORE scoring function to determine the top 1000 hits. Visual inspection of the top conformations confirmed that a consensus structure as shown in Fig. 1A was evident. The molecular models were displayed with the PyMOL software (DeLano Scientific, San Carlos, CA).

4.4. Synthesis and compound characterization

4.4.1. Compound characterization

New compounds were characterized by their physical and spectroscopic properties (mp, TLC, [α], IR, ESI–MS, ^{1}H, ^{13}C and ^{31}P NMR). Purity of synthetic compounds was assessed to be ≥95% by HPLC analysis (Agilent HP-1100) on an HC-C18 column (250 mm × 4.6 mm i.d., 5 μm particle size) using eluents at a flow rate of 1.0 mL/min with detection at 214-nm wavelength. Compounds **5** [29], **6** [28], **7** [29], **8f** [45], **9c** [29], **10c** [29], **3c** [29], **3e** [20] and **4c** [29] were identified by comparison with the physical and spectroscopic properties (mp, TLC, [α], IR, ESI–MS, ^{1}H, ^{13}C and ^{31}P NMR) as that reported previously.

4.4.2. Ethyl 4-acetamido-5-(tert-butoxycarbonyl)amino-3-(1-ethylpropoxy)-1-cyclohexene-1-carboxylate (**5**)

To a mixture of oseltamivir (0.75 g, 2.4 mmol) and $NaHCO_3$ (0.77 g, 9.14 mmol) in THF/H_2O (10 mL/10 mL) was added $(Boc)_2O$ (0.52 g, 2.38 mmol). The mixture was stirred for 2 h at room temperature, and concentrated under reduced pressure. The residue was diluted with CH_2Cl_2, and washed with water. The aqueous phase was extracted with CH_2Cl_2 (3×). The combined organic phase was dried over $MgSO_4$, filtered, and concentrated under reduced pressure to give compound **5** (1.0 g, 2.4 mmol). $C_{21}H_{36}N_2O_6$; colorless solid, mp 142–144 °C; TLC (EtOAc/hexane, 1:3) $R_f = 0.16$; ^{1}H NMR (400 MHz, $CDCl_3$) δ 6.77 (1H, s), 5.82 (1H, d, $J = 8.8$ Hz), 5.10 (1H, d, $J = 9.2$ Hz), 4.23–4.15 (2H, m), 4.08–4.01 (1H, m), 4.06–3.95 (1H, m), 3.82–3.73 (1H, m), 3.36–3.31 (1H, m), 2.96 (1H, dd, $J = 1.8$, 4.8 Hz), 2.31–2.24 (1H, m), 1.97 (3H, s), 1.57–1.45 (4H, m), 1.41 (9H, s), 1.28 (3H, t, $J = 7.2$ Hz), 0.91–0.85 (6H, m); ^{13}C NMR (100 MHz, $CDCl_3$) δ 170.1, 165.2, 155.7, 137.2, 128.8, 82.1, 79.5, 75.8, 61.0, 54.6, 49.3, 31.2, 28.6 (3×), 26.5, 26.0, 23.7, 14.6, 10.0, 9.7; HRMS calcd for $C_{21}H_{37}N_2O_6$: 413.2652, found: *m/z* 413.2658 $[M + H]^+$.

4.4.3. 4-Acetamido-5-(tert-butoxycarbonyl)amino-3-(1-ethylpropoxy)-1-cyclohexene-1-carboxylic acid (**6**)

Compound **5** (1.0 g, 2.4 mmol) was stirred with 1.0 M aqueous KOH (3.5 mL) in MeOH (6.6 mL) at room temperature for 2 h, and then neutralized with Dowex 50W × 8. The mixture was filtered, washed with MeOH, and concentrated under reduced pressure to give carboxylic acid **6** (0.63 g, 90%). $C_{19}H_{32}N_2O_6$; white solid, mp 195–197 °C; TLC (EtOAc/hexane, 2:1) $R_f = 0.10$; ^{1}H NMR (400 MHz, CD_3OD) δ 6.79 (1H, s), 4.11 (1H, d, $J = 8.4$ Hz), 3.88–3.83 (1H, m), 3.75–3.68 (1H, m), 3.41 (1H, t, $J = 5.6$ Hz), 2.71–2.66 (1H, m), 2.28–2.19 (1H, m), 1.96 (3H, s), 1.56–1.49 (4H, m), 1.44 (9H, s), 0.90–0.85 (6H, m); ^{13}C NMR (100 MHz, $CDCl_3$) δ 169.5, 168.1, 155.3, 135.0, 131.6, 81.0, 77.7, 75.4, 54.5, 49.3, 31.0, 28.4 (3×), 26.0, 25.4, 23.0, 9.6, 9.2; HRMS calcd for $C_{19}H_{33}N_2O_6$: 385.2339, found: *m/z* 385.2337 $[M + H]^+$.

4.4.4. 4-Acetamido-5-(tert-butoxycarbonyl)amino-3-(1-ethylpropoxy)-1-iodo-1-cyclohexene (**7**)

To a solution of carboxylic acid **6** (0.25 g, 0.65 mmol) in anhydrous CH_2Cl_2 (8 mL) were added Et_3N (0.14 mL, 0.98 mmol), HBTU (0.37 g, 0.98 mmol), and DMAP (catalytic amount). The mixture was stirred at room temperature for 30 min, and 3-hydroxy-4-methyl thiazolethione (0.13 g, 0.86 mmol) was added. The mixture was stirred for another 3 h at room temperature, and concentrated under reduced pressure. The residue was purified by flash chromatography on a silica gel column (EtOAc/hexane, 1:1–2:1) to afford an intermediate Barton ester (0.3 g, 90%).

A solution containing the intermediate Barton ester (0.3 g, 0.58 mmol) and trifluoroethyl iodide (2 mL, 1.5 mmol) in anhydrous CH_2Cl_2 (0.3 M, 2 mL) was irradiated by 500 W lamp at room temperature for 0.5 h. The mixture was concentrated under reduced pressure, and purified by flash chromatography on a silica gel column (EtOAc/hexane, 1:3 to 1:1) to afford compound **7** (164 mg, 0.35 mmol, 54% overall yield). $C_{18}H_{31}IN_2O_4$; pale yellow solid, mp 161–163 °C; TLC (EtOAc/hexane, 1:1) $R_f = 0.5$; ^{1}H NMR (400 MHz, $CDCl_3$) δ 6.31 (1H, s), 5.61 (1H, d, $J = 16.4$ Hz), 5.26 (1H, d, $J = 8.8$ Hz), 4.08 (1H, q, $J = 9.6$ Hz), 3.84–3.75 (2H, m), 3.28 (1H, t, $J = 5.6$ Hz), 2.86 (1H, dd, $J = 4.4$, 5.8 Hz), 2.60 (1H, dd, $J = 1.7$, 4.08 Hz), 1.98 (3H, s), 1.54–1.41 (13H, m), 0.90–0.85 (6H, m); ^{13}C NMR (100 MHz, $CDCl_3$) δ 170.7, 155.8, 138.0, 94.5, 82.0, 79.6, 77.5, 53.3, 50.5, 45.1, 28.4 (3×), 26.2, 25.8, 23.4, 9.7, 9.4; HRMS calcd for $C_{18}H_{32}IN_2O_4$: 467.1407, found: *m/z* 467.1403 $[M + H]^+$.

4.4.5. Di[3-(1H-indol-3-yl)propyl] phosphite (**8g**)

A mixture of 3-(1*H*-indol-3-yl)propan-1-ol (0.64 g, 3.6 mmol) and pyridine (0.43 g, 5.5 mmol) was added dropwise to a solution of phosphorus trichloride (0.25 g, 1.8 mmol) in CH_2Cl_2 (12.0 mL) at 0 °C. The mixture was stirred for 2 h, filtered, and rinsed with cyclohexane. The filtrate was concentrated, dissolved in EtOAc, and washed twice with brine. The organic layer was dried over $MgSO_4$, and concentrated under reduced pressure to give phosphite **8g** (0.44 g, 61% yield). $C_{22}H_{25}N_2O_3P$; pale yellow oil; TLC (EtOAc/hexane; 1:1) $R_f = 0.33$; ^{1}H NMR (400 MHz, $CDCl_3$) δ 7.94 (2H, br), 7.49 (2H, d, $J = 7.6$ Hz), 7.25 (2H, d, $J = 7.2$ Hz), 7.10 (2H, t, $J = 7.6$ Hz), 7.00–7.05 (2H, m), 6.86 (2H, d, $J = 1.6$ Hz), 6.75 (1H, d, $J = 692.4$ Hz), 4.01–4.04 (4H, m), 2.79 (4H, t, $J = 7.2$ Hz), 2.00 (4H, q, $J = 6.8$ Hz); ^{13}C NMR (100 MHz, $CDCl_3$) δ 136.2 (2×), 127.2 (2×), 121.8 (2×), 121.6 (2×), 119.1 (2×), 118.6 (2×), 114.6 (2×), 111.1 (2×), 65.2 (2×, d, $^2J_{C-P} = 6.1$ Hz), 30.7 (2×, d, $^3J_{C-P} = 6.8$ Hz), 21.0 (2×); ^{31}P NMR (162 MHz, $CDCl_3$) δ 9.1.

4.4.6. General procedure for the preparation of dialkyl tamiphosphor **9c**–**9g**

A mixture of iodocyclohexene **7** (130 mg, 0.28 mmol), phosphite diester (**8c**–**8g**, 0.28 mmol) and Et_3N (1.2 mL, 0.84 mmol) in anhydrous toluene (2.0 mL) was deoxygenated by bubbling with nitrogen for 10 min, and then added to tetrakis(-triphenylphosphine)palladium(0) (1 mg, 0.86 μmol) that was placed in a round-bottomed flask under nitrogen atmosphere. The resulting solution was gradually heated to 90 °C and maintained at this temperature for 3 h. The reaction mixture was filtered through a pad of Celite, and the filtrate was concentrated under reduced pressure to give yellow foam, which was purified by flash chromatography on a silica gel column (EtOAc/hexane = 1:1) to afford the desired phosphonate product (**9c**–**9g**).

4.4.7. Dibutyl (3R,4R,5S)-4-acetamido-5-tert-butoxycarbonylamino-3-(1-ethyl- propoxy)-1-cyclohexene-1-phosphonate (**9d**)

According to the general procedure, iodocyclohexene **7** (100 mg, 0.21 mmol) in anhydrous toluene (2.1 mL) was treated with dibutyl phosphite **8d** (60 mg, 0.32 mmol), Et_3N (0.66 mg, 0.64 mmol) and $(Ph_3P)_4Pd$ (10 mg, 8.6 μmol) at 90 °C for 12 h to afford phosphonate **9d** (73 mg, 64% yield). $C_{26}H_{49}N_2O_7P$; pale yellow solid, mp 159–161 °C; TLC (EtOAc/hexane, 1:1) R_f = 0.11; $[\alpha]_D^{24}$ −68.7 (c = 1, CH_2Cl_2); IR (film) 3349, 2961, 1683, 1567, 1297 cm^{-1}; ^1H NMR (400 MHz, $CDCl_3$) δ 6.52 (1H, d, J = 21.6 Hz), 6.15 (1H, d, J = 9.2 Hz), 5.22 (1H, d, J = 9.2 Hz), 3.87–4.04 (6H, m), 3.72–3.77 (1H, m), 3.28–3.31 (1H, m), 2.51–2.58 (1H, m), 2.13–2.21 (1H, m), 1.92 (3H. s), 1.55–1.63 (8H, m), 1,29–1.47 (13H, m), 0.78–0.90 (12H, m); ^{13}C NMR (100 MHz, $CDCl_3$) δ 170.6, 155.9, 141.1 (d, $^2J_{C-P}$ = 6.8 Hz), 127.1 (C-1, d, $^1J_{C-P}$ = 181 Hz), 82.0, 79.4, 75.9, 75.7, 65.7, 65.6 (d, $^3J_{C-P}$ = 7.6 Hz), 54.1, 49.0 (d, $^2J_{C-P}$ = 14.4 Hz), 32.48, 32.46, 32.42, 31.0 (d, $^3J_{C-P}$ = 6.9 Hz), 28.3 (3×), 26.1, 26.0, 23.3, 18.8, 13.6, 9.5, 9.2; ^{31}P NMR (162 MHz, $CDCl_3$) δ 16.9; HRMS calcd for $C_{26}H_{49}N_2NaO_7P$: 555.3175, found: m/z 555.3138 $[M + Na]^+$.

4.4.8. Dihexyl (3R,4R,5S)-4-acetamido-5-tert-butoxycarbonylamino-3-(1-ethyl- propoxy)-1-cyclohexene-1-phosphonate (**9e**)

According to the general procedure, iodocyclohexene **7** (80 mg, 0.17 mmol) in anhydrous toluene (1.7 mL) was treated with dihexyl phosphite **8e** (51 mg, 0.20 mmol), Et_3N (70 μL, 0.51 mmol) and $(Ph_3P)_4Pd$ (10 mg, 8.6 μmol) at 90 °C for 12 h to afford phosphonate **9e** (71 mg, 70% yield). $C_{30}H_{57}N_2O_7P$; yellow oil; TLC (EtOAc/hexane, 1:1) R_f = 0.38–0.43; $[\alpha]_D^{23}$ −66.5 (c = 1, CH_2Cl_2); IR (film) 3287, 2959, 1687, 1655, 1561, 1366, 1297, 1253, 1173 cm^{-1}; ^1H NMR (400 MHz, $CDCl_3$) δ 6.59 (1H, d, J = 8.8 Hz), 6.44 (1H, d, J = 21.6 Hz), 5.35 (1H, d, J = 9.2 Hz), 3.79–3.97 (6H, m), 3.64–3.74 (1H, m), 3.24–3.29 (1H, m), 2.47–2.51 (1H, m), 2.11–2.17 (1H, m), 1.86 (3H, s), 1.10–1.58 (29H, m), 0.74–0.79 (12H, m); ^{13}C NMR (100 MHz, $CDCl_3$) δ 170.5, 155.8, 141.0 (d, $^2J_{C-P}$ = 7.6 Hz), 126.9 (C-1, d, $^1J_{C-P}$ = 180 Hz), 81.9, 79.1, 75.6, 75.4, 65.9, 65.8 (d, $^2J_{C-P}$ = 3.1 Hz), 54.0, 49.0, 48.9 (d, $^2J_{C-P}$ = 14.4 Hz), 31.2, 30.8 (d, $^3J_{C-P}$ = 9.1 Hz), 30.34, 30.31, 30.28, 30.25, 28.2 (3×), 26.0, 25.5, 25.1, 23.1, 22.4, 13.9, 9.4, 9.1; ^{31}P NMR (162 MHz, $CDCl_3$) δ 17.9; HRMS calcd for $C_{30}H_{58}N_2O_7P$: 587.3825, found: m/z 587.3824 $[M + H]^+$.

4.4.9. Di(3-phenylprop-1-yl) (3R,4R,5S)-4-acetamido-5-tert-butoxycarbonylamino-3-(1-ethylpropoxy)-1-cyclohexene-1-phosphonate (**9f**)

According to the general procedure, iodocyclohexene **7** (100 mg, 0.21 mmol) in anhydrous toluene (2.1 mL) was treated with dioctyl phosphite **8f** (75 mg, 0.24 mmol), Et_3N (100 μL, 0.64 mmol) and $(Ph_3P)_4Pd$ (1.0 mg, 0.86 μmol) at 90 °C for 3 h to afford phosphonate **9f** (120 mg, 86% yield). $C_{36}H_{53}N_2O_7P$; pale yellow solid, mp 112–114 °C; TLC (EtOAc/hexane, 1:1) R_f = 0.47; $[\alpha]_D^{23}$ −79.6 (c = 1, CH_2Cl_2); IR (film) 3283, 2963, 2934, 1686, 1657, 1566, 1533, 1454, 1367, 1297, 1253, 1013 cm^{-1}; ^1H NMR (400 MHz, $CDCl_3$) δ 7.15–7.28 (10H, m), 6.59 (1H, d, J = 22.0 Hz), 5.79 (1H, d, J = 9.2 Hz), 5.01 (1H, d, J = 8.8 Hz), 3.95–4.08 (6H, m), 3.88–3.90 (1H, m), 3.76–3.80 (1H, m), 3.29–3.32 (1H, m), 2.59 (1H, dt, J = 17.6, 6.4 Hz), 2.13–2.20 (1H, m), 1.93–2.04 (8H, m), 1.44–1.52 (6H, m), 1.41 (9H, s), 0.84–0.88 (6H, m); ^{13}C NMR (100 MHz, $CDCl_3$) δ 170.7, 156.1, 141.7, 140.7, 132.0, 131.9, 131.85, 131.8, 128.4 (2×), 128.3 (2×), 127.2 (C-1, d, $^1J_{C-P}$ = 216.6 Hz), 125.9 (2×), 82.2, 79.7, 76.3, 76.1, 65.3 (d, $^2J_{C-P}$ = 5.4 Hz), 65.2, 54.5, 49.2 (d, $^2J_{C-P}$ = 15.2 Hz), 32.1(d, $^3J_{C-P}$ = 6.8 Hz), 31.8, 31.4, 31.3, 29.7, 28.4 (3×), 26.2, 25.6, 23.4, 9.7, 9.3; ^{31}P NMR (162 MHz, $CDCl_3$) δ 18.1; HRMS calcd for $C_{36}H_{52}N_2O_7P$: 655.3512, found: m/z 655.3518 $[M - H]^-$.

4.4.10. Di[3-(1H-indol-3-yl)propyl] (3R,4R,5S)-4-acetamido-5-tert-butoxycarbonylamino-3-(1-ethylpropoxy)-1-cyclohexene-1-phosphonate (**9g**)

According to the general procedure, iodocyclohexene **7** (130 mg, 0.28 mmol) in anhydrous toluene (2.0 mL) was treated with di[3-(1*H*-indol-3-yl)propyl] phosphite **8g** (110 mg, 0.28 mmol), Et_3N (1.2 mL, 0.84 mmol) and $(Ph_3P)_4Pd$ (1 mg, 0.86 μmol) at 90 °C for 3 h to afford phosphonate **9g** (122 mg, 72% yield) after flash chromatography on a silica gel column by elution with EtOAc/hexane (1:1) and CH_2Cl_2/MeOH (10:1). $C_{40}H_{55}N_4O_7P$; pale yellow oil; TLC (EtOAc/hexane, 1:1) R_f = 0.12; $[\alpha]_D^{24}$ −79.9 (c = 1, CH_2Cl_2); IR (film) 3285, 2965, 2930, 1687, 1530, 1456, 1367, 1258, 1230, 1168, 1012 cm^{-1}; ^1H NMR (400 MHz, $CDCl_3$) δ 8.83 (1H, s), 8.59 (1H, s), 7.53–7.56 (2H, m), 7.33 (2H, t, J = 8.4 Hz), 7.05–7.17 (4H, m), 6.90–6.96 (2H, m), 6.52 (1H, d, J = 21.6 Hz), 5.81 (1H, d, J = 9.2 Hz), 4.57 (1H, d, J = 9.6 Hz), 4.11 (1H, q, J = 6.8 Hz), 3.92–4.06 (4H, m), 3.75–3.82 (1H, m), 3.70 (1H, br), 3.58 (1H, dd, J = 10.0, 5.2 Hz), 3.20–3.25 (1H, m), 2.75–2.90 (4H, m), 2.34 (1H, dt, J = 19.6, 6.4 Hz), 2.04 (3H, s), 1.98 (4H, t, J = 8.0 Hz), 1.43–1.47 (9H, m), 1.23–1.33 (4H, m), 0.82–0.88 (6H, m); ^{13}C NMR (100 MHz, $CDCl_3$) δ 170.8, 156.3, 142.3, 136.3, 136.2, 131.9, 131.8, 127.9 (C-1, d, $^1J_{C-P}$ = 84.4 Hz), 127.2, 127.1, 121.7, 121.6, 118.6, 118.56, 114.3, 114.1, 111.4, 111.2, 82.2, 79.7, 76.4, 65.3 (d, $^2J_{C-P}$ = 5.4 Hz), 60.4, 55.1, 48.7 (d, $^2J_{C-P}$ = 15.2 Hz), 30.3 (d, $^3J_{C-P}$ = 6.8 Hz), 29.9, 29.8, 28.4 (3×), 26.1, 25.5, 23.5, 21.1, 21.0, 20.8, 14.3, 9.7, 9.2; ^{31}P NMR (162 MHz, $CDCl_3$) δ 18.1. HRMS (negative mode) calcd for $C_{40}H_{54}N_4O_7P$: 733.3730, found: m/z 733.3745 $[M - H]^-$.

4.4.11. General procedure for the preparation of guanidino tamiphosphor dialkyl esters **10c**–**10f**

A solution of phosphonate compound (**9c**–**9f**, 0.073 mmol) in anhydrous CH_2Cl_2 (1.0 mL) was cooled to 0 °C in ice-bath, and TFA (0.055 mL, 0.73 mmol) was added. The mixture was stirred for 2 h at room temperature, and concentrated under reduced pressure to give brown liquid of intermediate amine, which was treated with, *N*,*N*′-bis-(*tert*-butoxycarbonyl)-*S*-methylisothiourea (14 mg, 0.049 mmol), $HgCl_2$ (13.3 mg, 0.049 mmol) and triethylamine (0.018 mL, 0.14 mmol) in CH_2Cl_2 (1 mL). The mixture was stirred at room temperature for 2 h, added 1 M HCl (5 mL), and extracted with CH_2Cl_2 (5 mL × 3). The organic phase was dried over $MgSO_4$, filtered, and concentrated under reduced pressure. The residual oil was purified by flash column chromatography (CH_2Cl_2/MeOH = 20:1) to yield the desired guanidino-tamiphosphor dialkyl ester (**10c**–**10f**).

4.4.12. Dibutyl (3R,4R,5S)-4-acetamido-5-[N^2,N^3-bis(tert-butoxycarbonyl)guanidino]-3-(1-ethylpropoxy)-1-cyclohexene-1-phosphonate (**10d**)

According to the general procedure, compound **9d** (150 mg, 0.28 mmol) was treated with TFA (0.32 mL, 4.2 mmol) in CH_2Cl_2

(0.3 mL) at room temperature for 1 h to remove the *t*-Boc protecting groups. The amine product in CH_2Cl_2 (1 mL) was treated with *N*,*N*′-bis-(*tert*-butoxycarbonyl)-*S*-methylisothiourea (98 mg, 0.33 mmol), $HgCl_2$ (92 mg, 0.32 mmol) and Et_3N (0.12 mL, 0.84 mmol) at room temperature for 3 h to yield compound **10d** (136 mg, 72% yield). $C_{32}H_{59}N_4O_9P$; colorless oil; TLC (CH_2Cl_2/MeOH, 20:1) R_f = 0.63; $[\alpha]_D^{23}$ −57.6 (c = 1, CH_2Cl_2); IR (film) 3272, 2963, 1730, 1639, 1416, 1367, 1307, 1249 cm^{-1}; ^1H NMR (400 MHz, $CDCl_3$) δ 11.35 (1H, s), 8.56 (1H, d, J = 8.0 Hz), 6.59 (1H, d, J = 21.6 Hz), 6.34 (1H, d, J = 9.2 Hz), 4.34–4.38 (1H, m), 4.12 (1H, q, J = 8.4 Hz), 3.92–4.03 (5H, m), 3.30–3.34 (1H, m), 2.59–2.66 (1H, m), 2,25–2.32 (1H, m), 1.90 (3H, s), 1.23–1.66 (30H, m), 0.82–0.94 (12H, m); ^{13}C NMR (100 MHz, $CDCl_3$) δ 170.1, 162.8, 156.6, 152.3, 141.8 (d, $^2J_{C-P}$ = 6.8 Hz), 126.3 (C-1, d, $^1J_{C-P}$ = 181 Hz), 83.5, 82.5, 79.5, 76.5, 76.2, 65.8, 65.75, 65.6 (d, $^2J_{C-P}$ = 6.1 Hz), 54.4, 48.2 (d, $^2J_{C-P}$ = 14.4 Hz), 32.51, 32.45, 30.9 (d, $^3J_{C-P}$ = 9.2 Hz), 28.3 (3×), 28.1 (3×), 26.1, 25.6, 23.3, 18.8, 13.7, 9.7, 9.3; ^{31}P NMR (162 MHz, $CDCl_3$) δ 17.9; HRMS calcd for $C_{32}H_{58}N_4O_9P$: 673.3941, found: m/z 673.3951 $[M - H]^-$.

4.4.13. Dihexyl (3R,4R,5S)-4-acetamido-5-[N^2,N^3-bis(tert-butoxycarbonyl)guanidino]-3-(1-ethylpropoxy)-1-cyclohexene-1-phosphonate (**10e**)

According to the general procedure, compound **9e** (85 mg, 0.14 mmol) was treated with TFA (0.11 mL, 1.4 mmol) in CH_2Cl_2 (1.0 mL) at room temperature for 1 h to remove the *t*-Boc protecting groups. The amine product in CH_2Cl_2 (0.5 mL) was treated with *N*,*N*′-bis-(*tert*-butoxycarbonyl)-*S*-methylisothiourea (46 mg, 0.16 mmol), $HgCl_2$ (43 mg, 0.16 mmol) and Et_3N (0.06 mL, 0.43 mmol) at room temperature for 3 h to yield compound **10e** (63 mg, 60% yield). $C_{36}H_{67}N_4O_9P$; colorless oil; TLC (EtOAc/hexane, 1:1) R_f = 0.32; $[\alpha]_D^{22}$ −59.6 (c = 1, CH_2Cl_2); IR (film) 3449, 3277, 2960, 2930, 1730, 1639, 1611, 1561, 1418, 1368, 1153 cm^{-1}; ^1H NMR (400 MHz, $CDCl_3$) δ 11.36 (1H, s), 8.58 (1H, d, J = 8.0 Hz), 6.59 (1H, d, J = 21.6 Hz), 6.42 (1H, d, J = 9.2 Hz), 434–4.40 (1H, m), 4.11–4.16 (1H, m), 3.91–4.09 (5H, m), 3.29–3.34 (1H, m), 2.60–2.67 (1H, m), 2.25–2.33 (1H, m), 1.90 (3H, s), 1.22–1.65 (38H, m), 0.80–0.89 (12H, m); ^{13}C NMR (100 MHz, $CDCl_3$) δ 170.1, 162.8, 156.7, 152.4, 141.9 (d, $^2J_{C-P}$ = 7.6 Hz), 126.2 (C-1, d, $^1J_{C-P}$ = 182 Hz), 83.5, 82.5, 79.5, 76.5, 76.3, 66.2, 66.1, 66.0 (d, $^2J_{C-P}$ = 6.1 Hz), 54.5, 48.3 (d, $^2J_{C-P}$ = 14.4 Hz), 31.4, 31.0 (d, $^3J_{C-P}$ = 9.9 Hz), 30.5, 30.4, 29.7, 28.3 (3×), 28.1 (3×), 26.1, 25.7, 25.28, 25.26, 23.3, 22.6, 14.1, 9.7, 9.3; ^{31}P NMR (162 MHz, $CDCl_3$) δ 17.9; HRMS calcd for $C_{36}H_{68}N_4O_9P$: 731.4724, found: m/z 731.4734 $[M + H]^+$.

4.4.14. Di(3-phenylprop-1-yl) (3R,4R,5S)-4-acetamido-5-[N^2,N^3-bis(tert-butoxycarbonyl)guanidino]-3-(1-ethylpropoxy)-1-cyclohexene-1-phosphonate (**10f**)

According to the general procedure, compound **9f** (110 mg, 0.15 mmol) was treated with TFA (0.11 mL, 1.5 mmol) in CH_2Cl_2 (0.5 mL) at room temperature for 1 h to remove the *t*-Boc protecting groups. The amine product in CH_2Cl_2 (1.7 mL) was treated with *N*,*N*′-bis-(*tert*-butoxycarbonyl)-*S*-methylisothiourea (48 mg, 0.17 mmol), $HgCl_2$ (45 mg, 0.17 mmol) and Et_3N (0.07 mL, 0.46 mmol) at room temperature for 3 h to yield compound **10f** (98 mg, 75% yield). $C_{42}H_{63}N_4O_9P$; pale yellow oil; TLC (EtOAc/hexane, 1:1) R_f = 0.34; $[\alpha]_D^{23}$ −43.7 (c = 1, CH_2Cl_2); IR (film) 2973, 2934, 1789, 1729, 1639, 1416, 1368, 1307, 1229, 1146 cm^{-1}; ^1H NMR (400 MHz, $CDCl_3$) δ 11.43 (1H, s), 8.70 (1H, d, J = 8.4 Hz), 7.22–7.35 (10H, m), 6.70 (1H, d, J = 22.0 Hz), 6.46 (1H, d, J = 9.2 Hz), 4.47–4.55 (1H, m), 4.17–4.24 (1H, m), 4.03–4.13 (5H, m), 3.39 (1H, m), 2.76 (4H, t, J = 7.6 Hz), 2.68–2.72 (1H, m), 2.32–2.38 (1H, m), 2.05 (4H, t, J = 7.2 Hz), 2.00 (3H, s), 1.99–1.70 (22H, m), 0.90–0.97 (6H, m); ^{13}C NMR (100 MHz, $CDCl_3$) δ 170.8, 162.8, 157.0, 152.6, 142.3 (d, $^2J_{C-P}$ = 7.6 Hz), 140.9, 132.2, 132.1, 128.6, 128.4, 126.1, 126.3 (C-1, d, $^1J_{C-P}$ = 182 Hz), 83.8, 82.6, 80.1, 79.7, 77.3, 76.3, 76.1, 67.1, 65.5, 65.4, 65.3 (d, $^2J_{C-P}$ = 6.1 Hz), 54.4, 48.2 (d, $^2J_{C-P}$ = 14.4 Hz), 32.0 (d, $^3J_{C-P}$ = 6.8 Hz), 31.7, 30.9, 30.8, 28.3 (3×), 28.2, 28.01 (3×), 27.96, 26.1, 25.6, 23.3, 9.7, 9.2; ^{31}P NMR (162 MHz, $CDCl_3$) δ 18.1; HRMS calcd for $C_{42}H_{64}N_4O_9P$: 799.4411, found: m/z 799.4413 $[M + H]^+$.

4.4.15. General procedure for the preparation of tamiphosphor monoesters **3c**–**3g** and guanidino-tamiphosphor monoesters **4c**–**4f**

A solution of tamiphosphor dialkyl ester (**9c**–**9g**, 0.18 mmol) in CH_2Cl_2 (0.13 mL) was treated with TFA (0.14 mL, 19 mmol) at room temperature for 2 h. The mixture was concentrated under reduced pressure, dissolved in 1,4-dioxane (2.6 mL), and added 1 M $KOH_{(aq)}$ (1.8 mL). The mixture was stirred at 40 °C for 24–60 h (monitored by ^1H NMR), and Dowex 50W × 8 resin was added to neutralize the solution in MeOH for 5 min. The mixture was filtered, and the filtrate was concentrated under reduced pressure. The crude product was purified by DE-50 anion exchange resin and C-18 gel columns. The product was dissolved in aqueous NH_4OH (2 mL, 16 M)/MeOH (5 mL), stirred at room temperature for 0.5 h, and then lyophilized to afford tamiphosphor monoester **3c**–**3g**. Compounds **4c**–**4f** were similarly prepared from guanidino-tamiphosphor dialkyl esters **10c**–**10f** (0.13 mmol) by the procedure similar to that for **3c**–**3g**.

4.4.16. Monobutyl (3R,4R,5S)-4-acetamido-5-amino-3-(1-ethylpropoxy)-1-cyclohexene-1-phosphonate (**3d**)

According to the general procedure, compound **9d** (100 mg, 0.18 mmol) in CH_2Cl_2 (0.13 mL) was treated with TFA (0.14 mL, 19 mmol) to give crude amino product, which was dissolved in 1,4-dioxane (2.6 mL) and treated with 1 M aqueous KOH (1.8 mL) at 40 °C for 36 h to afford compound **3d** (47 mg, 66% yield) as the ammonium salt. The purity of product **3d** was 95.2% as shown by HPLC on an HC-C18 column (Agilent, 4.6 × 250 mm, 5 μm) with elution of MeOH/H_2O (1:1), t_R = 6.2 min (UV detection at 214 nm wavelength). $C_{17}H_{33}N_2O_5P$; white solid; mp 227–229 °C; TLC (2-propanol/H_2O/NH_4OH, 10:2:3) R_f = 0.61; $[\alpha]_D^{22}$ −9.8 (c = 0.55, MeOH); IR (film) 3484, 3315, 2962, 2875, 1636, 1557, 1459, 1397, 1299, 1182, 1059, 1032 cm^{-1}; ^1H NMR (400 MHz, CD_3OD) δ 8.19 (1H, d, J = 8.4 Hz), 6.39 (1H, d, J = 18.4 Hz), 4,10 (1H, d, J = 7.6 Hz), 3.96 (2H, q, J = 6.4 Hz), 3.79 (2H, t, J = 6.4 Hz), 3.36–3.45 (1H, m), 2.78 (1H, dt, J = 16.8, 6.8 Hz), 2.35–2.42 (1H, m), 2.03 (3H,s), 1.38–1.64 (8H, m), 0.87–0.97 (9H, m); ^{13}C NMR (100 MHz, CD_3OD) δ 174.8, 136.4 (d, $^2J_{C-P}$ = 7.2 Hz), 132.6 (C-1, d, $^1J_{C-P}$ = 171 Hz), 83.4, 76.6 (d, $^3J_{C-P}$ = 5.7 Hz), 65.5 (d, $^2J_{C-P}$ = 171 Hz), 54.8, 51.6 (d, $^3J_{C-P}$ = 13.5 Hz), 34.3 (d, $^2J_{C-P}$ = 6.9 Hz), 30.8 (d, $^3J_{C-P}$ = 10.7 Hz), 27.5, 26.8, 23.3, 20.3, 14.3, 10.0, 9.7; ^{31}P NMR (162 MHz, CD_3OD) δ 12.2; HRMS calcd for $C_{17}H_{32}N_2O_5P$: 375.2049, found: m/z 375.2051 $[M + H]^+$.

4.4.17. Mono(3-phenylprop-1-yl) (3R,4R,5S)-4-acetamido-5-amino-3-(1-ethylpropoxy)-1-cyclohexene-1-phosphonate (**3f**)

According to the general procedure, compound **9f** (60 mg, 0.091 mmol) in CH_2Cl_2 (0.70 mL) was treated with TFA (0.07 mL, 1.3 mmol) to give crude amino product, which was dissolved in 1,4-dioxane (0.1 mL) and treated with 1 M aqueous KOH (0.91 mL) at 25 °C for 48 h to afford compound **3f** (25 mg, 63% yield) as the ammonium salt. The purity of product was >99% as shown by HPLC on an HC-C18 column (Agilent, 4.6 × 250 mm, 5 μm) with elution of MeOH/H_2O (40:60), t_R = 7.9 min (UV detection at 214 nm wavelength). $C_{22}H_{35}N_2O_5P$; white solid, mp 229–231 °C; TLC (2-propanol/H_2O/NH_4OH, 10:2:3) R_f = 0.74; $[\alpha]_D^{22}$ −37.0 (c = 0.2, MeOH); IR (film) 3445, 2964, 2939, 1455, 1375, 1296, 1060, 1030 cm^{-1}; ^1H NMR (400 MHz, CD_3OD) δ 8.19 (1H, d, J = 8.8 Hz), 7.12–7.26 (5H, m), 6.40 (1H, d, J = 18.8 Hz), 4,10 (1H, d, J = 8.0 Hz), 3.93–3.99 (1H, m), 3.82 (3H, q, J = 6.4 Hz), 3.36–3.44 (2H, m), 2.80 (1H, dt, J = 16.8, 7.2 Hz), 2.71 (2H, t, J = 8.0 Hz), 2.37–2.44 (1H, m),

2.03 (3H, s), 1.90–1.92 (2H, m), 1.46–1.58 (4H, m), 0.87–0.91 (6H, m); ^{13}C NMR (100 MHz, CD_3OD) δ 174.9, 143.2, 136.7 (2×), 129.62 (2×), 128.27 (C-1, d, $^1J_{C-P} = 254$ Hz), 83.5, 76.7, 76.5, 65.2, 54.9, 51.6 (d, $^2J_{C-P} = 12.9$ Hz), 34.1 (d, $^3J_{C-P} = 6.0$ Hz), 33.3, 31.0, 30.9, 27.5, 26.8, 23.3, 10.1, 9.7; ^{31}P NMR (162 MHz, CD_3OD) δ 12.3; HRMS calcd for $C_{22}H_{36}N_2O_5P$: 439.2362, found: *m/z* 439.2361 $[M + H]^+$.

4.4.18. Mono[(1H-3-Indol-3-yl)propyl] (3R,4R,5S)-4-acetamido-5-amino-3-(1-ethylpropoxy)-1-cyclohexene-1-phosphonate (**3g**)

According to the general procedure, compound **9g** (55 mg, 0.075 mmol) in CH_2Cl_2 (1.0 mL) was treated with TFA (0.055 mL, 0.75 mmol) to give crude amino product, which was dissolved in 1,4-dioxane (0.75 mL) and treated with 1 M aqueous KOH (0.75 mL) at 25 °C for 48 h to afford compound **3g** (15 mg, 43%) as the ammonium salt. $C_{24}H_{36}N_3O_5P$; TLC (2-propanol/H_2O/NH_4OH, 7:2:3) R_f = 0.71; ^{1}H NMR (400 MHz, CD_3OD) δ 7.52 (1H, d, J = 8.0 Hz), 7.30 (1H, d, J = 8.4 Hz), 6.95–7.11 (3H, m), 6.40 (1H, d, J = 19.2 Hz), 4.05 (1H, d, J = 7.6 Hz), 3.85–3.96 (3H, m), 3.61–3.66 (1H, m), 3.46–3.50 (1H, m), 2.75–2.93 (3H, m), 2.34–2.41 (1H, m), 1.91–2.08 (5H, m), 1.47–1.55 (4H, m), 0.80–0.90 (6H, m); ^{31}P NMR (162 MHz, $CDCl_3$) δ 12.4; HRMS calcd for $C_{24}H_{37}N_3O_5P$: 476.2308, found: *m/z* 476.2308 $[M - H]^-$.

4.4.19. Monobutyl (3R,4R,5S)-4-acetamido-3-(1-ethylpropoxy)-5-guanidino-1-cyclohexene-1-phosphonate (**4d**)

According to the general procedure, compound **10d** (100 mg, 0.15 mmol) in CH_2Cl_2 (0.15 mL) was treated with TFA (0.17 mL, 22 mmol) to give crude gaunidino product, which was dissolved in EtOH–THF (1.5 mL/1.5 mL) and treated with 1 M aqueous KOH (1.8 mL) at 40 °C for 36 h to afford compound **4d** (32 mg, 52% yield) as the ammonium salt. The purity of product **4d** was >99% as shown by HPLC on an HC-C18 column (Agilent, 4.6 × 250 mm, 5 μm) with elution of MeOH/H_2O (1:1), t_R = 5.9 min (UV detection at 214 nm wavelength). $C_{18}H_{35}N_4O_5P$; white solid; mp 247–249 °C; TLC (2-propanol/H_2O/NH_4OH, 10:2:3) R_f = 0.57; $[\alpha]_D^{22}$ −8.2 (c = 0.2, MeOH); IR (film) 3541, 3172, 1800, 1706, 1667, 1403, 1247, 1182, 1059, 1020 cm^{-1}; ^{1}H NMR (400 MHz, CD_3OD) δ 6.42 (1H, d, J = 19.2 Hz), 4.37 (1H, d, J = 8.0 Hz), 3.99–4.05 (1H, m), 3.82–3.95 (3H, m), 3.61–3.66 (1H, m), 2.76–2.84 (1H, m), 2.42–2.48 (1H, m), 2.15 (3H, s), 1.40–1.75 (8H, m), 0.99–1.04 (6H, m), 0.96 (3H, t, J = 7.2 Hz); ^{13}C NMR (100 MHz, CD_3OD) δ 174.3, 158.7, 136.2 (d, $^2J_{C-P} = 6.4$ Hz), 133.7 (C-1, d, $^1J_{C-P} = 171$ Hz), 83.4, 77.0 (d, $^3J_{C-P} = 19.2$ Hz), 65.5 (d, $^2J_{C-P} = 5.0$ Hz), 56.0, 52.3 (d, $^3J_{C-P} = 12.8$ Hz), 34.3 (d, $^2J_{C-P} = 7.1$ Hz), 32.3 (d, $^3J_{C-P} = 9.2$ Hz), 27.5, 27.0, 23.0, 20.3, 14.3, 10.0, 9.9; ^{31}P NMR (162 MHz, CD_3OD) δ 13.0; HRMS calcd for $C_{18}H_{36}N_4O_5P$: 419.2423, found: *m/z* 419.2428 $[M + H]^+$.

4.4.20. Monohexyl (3R,4R,5S)-4-acetamido-3-(1-ethylpropoxy)-5-guanidino-1-cyclohexene-1-phosphonate (**4e**)

According to the general procedure, compound **10e** (180 mg, 0.23 mmol) in CH_2Cl_2 (0.30 mL) was treated with TFA (0.18 mL, 23 mmol) to give crude guanidino product, which was dissolved in 1,4-dioxane (7.6 mL) and treated with 1 M aqueous KOH (2.3 mL) at 25 °C for 60 h to afford compound **4e** (68 mg, 68% yield) as the ammonium salt. The purity of product was >96% as shown by HPLC on an HC-C18 column (Agilent, 4.6 × 250 mm, 5 μm) with elution of MeOH/H_2O (70:30), t_R = 8.7 min (UV detection at 214 nm wavelength). $C_{20}H_{39}N_4O_5P$; white solid, mp 245–247 °C; TLC (2-propanol/H_2O/NH_4OH, 10:2:3) R_f = 0.63; $[\alpha]_D^{22}$ −44.6 (c = 1, MeOH); IR(film) 3325, 2960, 2935, 2860, 1661, 1556, 1462, 1375, 1319, 1188, 1060, 1016 cm^{-1}; ^{1}H NMR (400 MHz, CD_3OD) δ 6.37 (1H, d, J = 19.2 Hz), 4.08 (1H, m), 3.92 (1H, t, J = 10 Hz), 3.74–3.83 (3H, m), 3.38–3.43 (1H, m), 2.64–2.71 (1H, m), 2.02–2.31 (1H, m), 1.98 (3H, s), 1.32–1.71 (12H, m), 0.88–0.94 (9H, m); ^{13}C NMR (100 MHz, CD_3OD) δ 174.2, 158.7, 136.5, 133.6 (C-1, d, $^1J_{C-P} = 171$ Hz), 83.4, 77.1 (d, $^2J_{C-P} = 18.9$ Hz), 65.9 (d, $^2J_{C-P} = 5.5$ Hz), 56.4, 52.4 (d, $^2J_{C-P} = 12.8$ Hz), 32.9, 32.7 (d, $^3J_{C-P} = 6.1$ Hz), 32.2, 31.7, 27.5, 27.0, 23.8, 23.0, 14.6, 10.1, 9.8; ^{31}P NMR (162 MHz, CD_3OD) δ 13.0; HRMS calcd for $C_{20}H_{38}N_4O_5P$: 445.2580, found: *m/z* 445.2581 $[M + H]^+$.

4.4.21. Mono(3-phenylpropyl) (3R,4R,5S)-4-acetamido-3-(1-ethylpropoxy)-5-guanidino-1-cyclohexene-1-phosphonate (**4f**)

According to the general procedure, compound **10f** (100 mg, 0.13 mmol) in CH_2Cl_2 (1.25 mL) was treated with TFA (0.11 mL, 1.3 mmol) to give crude guanidino product, which was dissolved in 1,4-dioxane (1.3 mL) and treated with 1 M aqueous KOH (1.3 mL) at 25 °C for 48 h to afford compound **4f** (60 mg, 55% yield). The purity of product **4f** was >99% as shown by HPLC on an HC-C18 column (Agilent, 4.6 × 250 mm, 5 μm) with elution of MeOH/H_2O (6:4), t_R = 7.5 min (UV detection at 214 nm wavelength). $C_{23}H_{37}N_4O_5P$; white solid; mp 252–254 °C; TLC (2-propanol/H_2O/NH_4OH, 10:2:3) R_f = 0.47; $[\alpha]_D^{22}$ −8.98 (c = 0.2, MeOH); IR (film) 3442, 2964, 1650, 1506, 1455, 1388, 1188, 1061 cm^{-1}; ^{1}H NMR (400 MHz, CD_3OD) δ 7.12–7.24 (5H, m), 6.39 (1H, d, J = 19.2 Hz), 4.08 (1H, d, J = 6.8 Hz), 3.93 (1H, dd, J = 9.6, 7.6 Hz), 3.74–3.85 (3H, m), 3.37–3.41 (1H, m), 2.72 (2H, t, J = 8.0 Hz), 2.67–2.72 (1H, m), 2.29–2.31 (1H, m), 1.98 (3H, s), 1.89–1.96 (2H, m), 1.47–1.56 (4H, m), 0.87–0.93 (6H, m); ^{13}C NMR (100 MHz, CD_3OD) δ 174.3, 158.7, 140.3, 136.3 (2×), 129.6 (2×), 128.3 (C-1, d, $^1J_{C-P} = 255$ Hz), 83.5, 77.1, 77.0, 65.1, 56.0, 52.4, 34.1, 33.3, 32.4 (2×), 27.5, 27.0, 23.0, 10.0, 9.9; ^{31}P NMR (162 MHz, CD_3OD) δ 13.0; HRMS calcd for $C_{23}H_{38}N_4O_5P$: 481.2580, found: *m/z* 481.2574 $[M + H]^+$.

4.5. Determination of octanol–buffer partition coefficients

The standard solutions of test compound in MeOH at various concentrations of 1.0, 0.5, 0.1, 0.05 and 0.01 mg/mL were measured by HPLC (Agilent 1100 series) on an HC-C18 column (5 μm porosity, 4.6 × 250 mm) using MeOH/H_2O (1:1) as the eluent and UV detector at λ = 214 nm. The integral area of the peak corresponding to the compound was used (average of triple experiments) to establish standard curve by Microsoft Excel.

To test compound partitioning, the respective test compounds (~1.0 mg) were placed in Eppendorf tube, and octanol (0.75 mL) and phosphate buffer saline (0.75 mL of 0.01 M solution, pH 7.4) were added. The solution was equilibrated at 37 °C using magnetic stirring at 1200 rpm for 24 h. The octanol and aqueous phases were then separated by centrifugation at 6000 rpm for 5 min. Each sample (25 μL) of aqueous layer was measured by HPLC. The concentration of drug in the aqueous phase was deduced by calibration with the above-established standard curve. Five replicates of each determination were carried out to assess reproducibility. From these data, the apparent octanol/buffer (pH 7.4) partition coefficient, $D_B = [Bt]_{oct}/[Bt]_{aq}$, is determined, where $[Bt]_{oct}$ and $[Bt]_{aq}$ are the concentrations of the drug in organic and aqueous phases, respectively.

4.6. Determination of influenza virus $TCID_{50}$

MDCK cells were obtained from American Type Culture Collection (Manassas, VA), and were grown in DMEM containing 10% fetal bovine serum and penicillin-streptomycin at 37 °C under 5% CO_2. The $TCID_{50}$ (50% tissue culture infectious dose) was determined by incubation of serially diluted influenza virus in 100 μL solution with 100 μL MDCK cells at 1 × 10^5 cells/mL in 96-well microplates. The infected cells were incubated at 37 °C under 5% CO_2 for 48–72 h and added to each wells with 100 μL per well of CellTiter 96 AQ_{ueous} Non-Radioactive Cell Proliferation Assay reagent (Promega). After incubation at 37 °C for 15 min, absorbance at 490 nm was read on a

plate reader. Influenza virus $TCID_{50}$ was determined using Reed–Muench method [46,47].

4.7. Determination of IC_{50} of neuraminidase inhibitors

The neuraminidase (NA) activity was measured using diluted allantoic fluid harvested from influenza virus infected embryonated eggs. A fluorometric assay was used to determine the NA activity with a fluorogenic substrate 2-(4-methylumbelliferyl)-α-D-*N*-acetylneuraminic acid (MUNANA; Sigma). For inhibition test, the compound of interest was incubated with diluted virus-infected allantoic fluid for 10 min at room temperature followed by the addition of 200 μM of substrate. The fluorescence of the released 4-methylumbelliferone was measured in Envision plate reader (Perkin–Elmer, Wellesley, MA) using excitation and emission wavelengths of 365 and 460 nm, respectively. Inhibitor IC_{50} values, i.e., the concentrations of the compound required for 50% inhibition of the NA, were measured in triplicate and determined from the dose–response curves by plotting the percent inhibition of NA activity versus inhibitor concentrations using Prism 5 (GraphPad Software, Inc., San Diego, CA).

4.8. Determination of EC_{50} and CC_{50} of neuraminidase inhibitors

The anti-influenza virus activities of NA inhibitors were measured by the EC_{50} values, i.e., the concentrations of the compound required for 50% protection of the influenza virus infection-mediated cytopathic effects (CPE). Fifty to 100 μL of diluted influenza virus (100 $TCID_{50}$) were mixed with equal volumes of NA inhibitors at varied concentrations. The mixtures were then used to infect 100 μL of MDCK cells at 1×10^5 cells/mL in 96-wells. After 48–72 h incubation at 37 °C under 5% CO_2, the CPE were determined with CellTiter 96 AQ_{ueous} Non-Radioactive Cell Proliferation Assay reagent as described above, or alternatively with 0.11 final percentage of neutral red for 2 h. Inhibitor EC_{50} value were measured in triplicate and determined by fitting the curve of percent CPE versus the concentrations of NA inhibitor using Graph Pad Prism 4.

The CC_{50} values (50% cytotoxic concentrations) of NA inhibitors to MDCK cells were determined by the procedures similar to the EC_{50} determination but without virus infection.

4.9. Cellular uptake and intestinal permeability

The MDCK type II cells (or Caco-2 cells) were continuously cultured in minimum essential medium supplemented with 0.11 g/L of sodium pyruvate, 1.5 g/L of sodium bicarbonate, 1% antibiotics (10,000 U/mL of penicillin, 10 mg/mL of streptomycin, and 25 μg/mL of amphotericin B), and 10% (for MDCK cells) or 20% (for Caco-2 cells) fetal bovine serum. The cells were routinely maintained in 75 cm^2 flasks at 37 °C in a 5% CO_2 and 95% humidity atmosphere. The culture medium was changed every 2 days. Cells were passaged after reaching 80% confluence. For subculturing, the cells were removed enzymatically (0.25% trypsin/EDTA), and subcultured in a T75 flask.

MDCK-II cells (5×10^4 cells) were grown on 6-well Nunclon Multidishes (9.6 cm^2 culture area, polystyrene, Nunc, Denmark) and were used for experiments 5 days after seeding. The experiments were conducted for time-dependency by incubating cells with 100 μg/mL of test compound (**4c**, **4e** or **4h**) for 30–120 min. The cells were then washed with 1.5 mL of ice-cold ECF buffer (122 mM NaCl, 3 mM KCl, 1.2 mM $MgSO_4$, 1.4 mM $CaCl_2$, 10 mM HEPES, 25 mM $NaHCO_3$, 0.4 mM K_2HPO_4, 10 mM D-glucose, pH 7.4) three times. The cells were then scrapped and sonicated in 1 mL methanol. After centrifugation (14,000 rpm, 25 °C, 10 min), the supernatant was removed and was evaporated to dryness by nitrogen gas. The residue was reconstituted with 100 μL of 50% methanol and an aliquot of 50 μL of sample was injected into a HPLC system. For protein assay, cells were solubilized in 1.0 mL of 1% Triton X-100, and the protein content of the cells was determined using the DC protein assay (Bio-Rad) with bovine serum albumin as the standard.

Caco-2 cells (5×10^4 cells) were seeded into millicell insert (4.2 cm^2 culture area, Millipore, Merck, USA), and the culture medium was changed every 2 days. The differentiation status of the monolayer was evaluated by measuring the transepithelial electrical resistance (TEER) (Millicell ERS epithelial volt-ohm meter, Millipore). Permeability was conducted until TEER values $> 300\ \Omega\ cm^2$. The experiments were conducted for time-dependency by incubating cells with 100 μg/mL of test compound for 15–120 min. First, the cells were rinsed three times with HBSS (1 mM $CaCl_2$, 0.5 mM $MgCl_2$, 5 mM KCl, 10 mM HEPES, 1 mM Na_2HPO_4, 140 mM NaCl, 5 mM D-glucose, pH 7.4). HBSS was loaded to the receiver side (1.5 mL) before incubation and the drug solution was added to donor side (apical (AP) side or basolateral (BL) side) (1.5 mL). An aliquot (200 μL) was collected from the receiver side (15, 30, 60, 120 min) and 50 μL was directly injected into HPLC. After each sampling, 200 μL of HBSS was supplemented to receiver side to maintain a constant volume of each side.

The HPLC system (Hitachi High-Technologies Co., Tokyo, Japan) consisted of a model L-2130 pump, a model L-2200 Autosampler, a model L-2400 ultraviolet detector, and a 4.6 mm × 250 mm Mightysil column (RP-18, 5 μm; MetaChem, CA, USA). The mobile phase consisted of 50% methanol in water (for **4c**) or 65% methanol in water (for **4e** and **4h**). The sample was analyzed at flow rate of 1.0 mL/min and was detected by ultraviolet at a wavelength of 214 nm. The lower quantitation limits were 500 ng/mL.

4.10. Pharmacokinetic study

Compound **4e** was administered as aqueous solutions in normal saline. Male ICR mice were purchased from BioLASCO Taiwan Co., Ltd. The compound was administered to mice as a single i.v. dose (0.25 mg/kg of body weight) or as a single oral dose (10 mg/kg). Plasma were prepared from tail lateral vein bleeds at 0.17, 0.33, 0.67, 1, 2, 4, 6, 8, and 12 h, and then stored at −70 °C. Deproteinized plasma samples were centrifuged for 10 min at 13,000 *g* and the supernatant was transferred to a plate for LC/MS/MS analysis.

The pharmacokinetic parameters were obtained using a pharmacokinetic program WinNonlin, fitting data to a non-compartmental model. The pharmacokinetic parameters including the area under the plasma concentration-versus-time curve (AUC) to the last sampling time, ($AUC_{0\rightarrow 12}$), to the time infinity ($AUC_{0\rightarrow\infty}$), the terminal-phase half-life ($T_{1/2}$), the maximum concentration of compound in plasma (C_{max}), the time of C_{max} (T_{max}), and the first order rate constant associated with the terminal portion of the curve (k) were estimated via linear regression of time versus log concentration. The total plasma clearance (CL) was calculated as dose/$AUC_{i.v.}$. The oral bioavailability (F) of the test compound by oral administration was calculated from the $AUC_{0-\infty}$ of the oral dose divided by the $AUC_{0\rightarrow\infty}$ of the i.v. dose.

4.11. Animal experiments for virus challenges

Female BALB/c mice (18–20 g) were obtained from Charles River Laboratories or National Laboratory Animal Center (Taiwan). The mice were quarantined for 48–72 h before use. The mice were anesthetized by intraperitoneal (i.p.) injection of zoletil (or ketamine/xylazine) and inoculated intranasally with 25 μL of infectious influenza virus. The test compounds were dissolved in sterile water,

and administered intranasally to mice at the indicated dosages by oral gavage (p.o.) twice daily for 5 days. Control mice received sterile water on the same schedule. Ten mice per test group were used throughout the studies. Four hours after the first dose of drug, mice were inoculated with influenza virus at 10 LD_{50}. Mice were observed daily for 14 days for survival, body weight and body temperature.

4.12. Statistical analysis

Kaplan–Meier survival curves were generated and compared by the Log-rank (Mantel–Cox) test using Prism 5.0b (GraphPad Software Inc.). Where statistical significance was seen, pairwise comparisons were made by the Gehan–Breslow–Wilcoxon test. Mean body weights were analyzed by ANOVA followed by Tukey's multiple comparison test using Prism 5.0b.

4.13. Ethical regulation of laboratory animals

This study was conducted in accordance with the approval of the Institutional Animal Care and Use Committee, Academia Sinica, Taiwan. The work was done in the BSL-3 Laboratory of Genomics Research Center, Academia Sinica, Taiwan.

Acknowledgments

We thank Academia Sinica and National Science Council for financial supports.

Appendix A. Supplementary data

Supplementary data associated with this article can be found in the online version, at http://dx.doi.org/10.1016/j.ejmech.2014.04.082. These data include MOL files and InChiKeys of the most important compounds described in this article.

References

[1] K. Das, J.M. Aramini, L.C. Ma, R.M. Krug, E. Arnold, Structures of influenza A proteins and insights into antiviral drug targets, Nat. Struct. Mol. Biol. 17 (2010) 530–538.
[2] H.M. Wise, E.C. Hutchinson, B.W. Jagger, A.D. Stuart, Z.H. Kang, N. Robb, L.M. Schwartzman, J.C. Kash, E. Fodor, A.D. Firth, J.R. Gog, J.K. Taubenburger, P. Digard, Identification of a novel splice variant form of the influenza A virus M2 ion channel with an antigenically distinct ectodomain, PLoS Pathog. 8 (2012) e1002998.
[3] A. Moscona, Neuraminidase inhibitors for influenza, N. Engl. J. Med. 353 (2005) 1363–1373.
[4] M. von Itzstein, W.-Y. Wu, G.B. Kok, M.S. Pegg, J.C. Dyason, B. Jin, T.V. Phan, M.L. Smythe, H.F. White, S.W. Oliver, P.M. Colman, J.N. Varghese, D.M. Ryan, J.M. Woods, R.C. Bethell, V.J. Hotham, J.M. Cameron, C.R. Penn, Rational design of potent sialidase-based inhibitors of influenza virus replication, Nature 363 (1993) 418–423.
[5] W. Lew, X. Chen, C.U. Kim, Discovery and development of GS 4104 (oseltamivir): an orally active influenza neuraminidase inhibitor, Curr. Med. Chem. 7 (2000) 663–672.
[6] R.J. Russell, L.F. Haire, D.J. Stevens, P.J. Collins, Y.P. Lin, G.-M. Blackurn, A.J. Hay, S.J. Gamblin, J.J. Skehel, The structure of H5N1 avian influenza neuraminidase suggests new opportunities for drug design, Nature 443 (2006) 45–49.
[7] J.M. Woods, R.C. Bethell, J.A. Coates, N. Healy, S.A. Hiscox, B.A. Pearson, D.M. Ryan, J. Ticehurst, J. Tilling, S.M. Walcott, 4-Guanidino-2,4-dideoxy-2,3-dehydro-*N*-acetylneuraminic acid is a highly effective inhibitor both of the sialidase (neuraminidase) and of growth of a wide range of influenza A and B viruses in vitro, Antimicrob. Agents Chemother. 37 (1993) 1473–1479.
[8] C.J. Dunn, K.L. Goa, Zanamivir: a review of its use in influenza, Drugs 58 (1999) 761–784.
[9] C.U. Kim, W. Lew, M.A. Williams, H. Wu, L. Zhang, X. Chen, P.A. Escarpe, D.B. Mendel, W.G. Laver, R.C. Stevens, Structure-activity relationship studies of novel carbocyclic influenza neuraminidase inhibitors, J. Med. Chem. 41 (1998) 2451–2460.
[10] K. McClellan, C.M. Perry, Oseltamivir: a review of its use in influenza, Drugs 61 (2001) 263–283.
[11] R.W. Sidwell, D.F. Smee, Peramivir (BCX-1812, RWJ-270201): potential new therapy for influenza, Expert Opin. Invest. Drugs 11 (2002) 859–869.
[12] S. Jain, A.M. Fry, Peramivir: another tool for influenza treatment? Clin. Infect. Dis. 52 (2011) 707–709.
[13] S. Kubo, T. Tomozawa, M. Kakuta, A. Tokumitsu, M. Yamashita, Laninamivir prodrug CS-8958, a long-acting neuraminidase inhibitor, shows superior anti-influenza virus activity after a single administration, Antimicrob. Agents Chemother. 54 (2010) 1256–1264.
[14] H. Ikematsu, N. Kawai, Laninamivir octanoate: a new long-acting neuraminidase inhibitor for the treatment of influenza, Expert Rev. Anti-Infect. Ther 9 (2011) 851–857.
[15] A.C. Schmidt, Antiviral therapy for influenza: a clinical and economic comparative review, Drugs 64 (2004) 2031–2046.
[16] E. De Clercq, Antiviral agents active against influenza A viruses, Nat. Rev. Drug Discov. 5 (2006) 1015–1025.
[17] K.A. Schug, W. Lindner, Noncovalent binding between guanidinium and anionic groups: focus on biological- and synthetic-based arginine/guanidinium interactions with phosph[on]ate and sulf[on]ate residues, Chem. Rev. 105 (2005) 67–114.
[18] J.-J. Shie, J.-M. Fang, S.-Y. Wang, K.-C. Tsai, Y.-S.E. Cheng, A.-S. Yang, S.-C. Hsiao, C.-Y. Su, C.-H. Wong, Synthesis of tamiflu and its phosphonate congeners possessing potent anti-influenza activity, J. Am. Chem. Soc. 129 (2007) 11892–11893.
[19] T.-J. Cheng, S. Weinheimer, E.B. Tarbet, J.-T. Jan, Y.-S.E. Cheng, J.-J. Shie, C.-L. Chen, C.-A. Chen, W.-C. Hsieh, P.-W. Huang, W.-H. Lin, S.-Y. Wang, J.-M. Fang, O.Y.-P. Hu, C.-H. Wong, Development of oseltamivir phosphonate congeners as anti-influenza agents, J. Med. Chem. 55 (2012) 8657–8670.
[20] B. Carbain, P.J. Collins, L. Callum, S.R. Martin, A.J. Hay, J. McCauley, H. Streicher, Efficient synthesis of highly active phospha-isosteres of the influenza neuraminidase inhibitor oseltamivir, ChemMedChem 4 (2009) 335–337.
[21] B. Carbain, S.R. Martin, P.J. Collins, P.B. Hitchcock, H. Streicher, Galactose-conjugates of the oseltamivir pharmacophore – new tools for the characterization of influenza virus neuraminidases, Org. Biomol. Chem. 7 (2009) 2570–2575.
[22] M. Stanley, S.R. Martin, M. Birge, B. Carbain, H. Streicher, Biotin-, fluorescein- and 'clickable' conjugates of phospha-oseltamivir as probes for the influenza virus which utilize selective binding to the neuraminidase, Org. Biomol. Chem. 9 (2011) 5625–5629.
[23] M. Stanley, N. Cattle, J. McCauley, S.R. Martin, A. Rashid, R.A. Field, B. Carbain, H. Streicher, 'TamiGold': phospha-oseltamivir-stabilised gold nanoparticles as the basis for influenza therapeutics and diagnostics targeting the neuraminidase (instead of the hemagglutinin), MedChemComm 3 (2012) 1373–1376.
[24] S. Rudrawar, J.C. Dyason, M.-A. Rameix-Welti, F.J. Rose, P.S. Kerry, R.J.M. Russell, S. van der Werf, R.J. Thomson, N. Naffakh, M. von Itzstein, Novel sialic acid derivatives lock open the 150-loop of an influenza A virus group-1 sialidase, Nat. Commun. 1 (113) (2010).
[25] R.E. Amaro, R.V. Swift, L. Votapka, W.W. Li, R.C. Walker, R.M. Bush, Mechanism of 150-cavity formation in influenza neuraminidase, Nat. Commun. 2 (388) (2011).
[26] R.E. Amaro, D.D.L. Minh, L.S. Cheng, W.M. Lindstrom, A.J. Olson, J.H. Lin, W.W. Li, J.A. McCammon, Remarkable loop flexibility in avian influenza N1 and its implications for antiviral drug design, J. Am. Chem. Soc. 129 (2007) 7764–7765.
[27] R.E. Amaro, X.L. Cheng, I. Ivanov, D. Xu, J.A. McCammon, Characterizing loop dynamics and ligand recognition in human- and avian-type influenza neuraminidases via generalized born molecular dynamics and end-point free energy calculations, J. Am. Chem. Soc. 131 (2009) 4702–4709.
[28] D.S. Gunasekera, Formal synthesis of tamiflu: conversion of tamiflu into tamiphosphor, Synlett 23 (2012) 573–576.
[29] J.-J. Shie, J.-M. Fang, C.-H. Wong, A concise and flexible synthesis of the potent anti-influenza agents tamiflu and tamiphosphor, Angew. Chem. Int. Ed. 47 (2008) 5788–5791.
[30] D.H.R. Barton, D. Crich, W.B. Motherwell, New and improved methods for the radical decarboxylation of acids, J. Chem. Soc. Chem. Commun. 17 (1983) 939–941.
[31] M.F. Saraiva, M.R.C. Couri, M. Le Hyaric, M.V. de Almeida, The Barton ester free-radical reaction: a brief review of applications, Tetrahedron 65 (2009) 3563–3572.
[32] L.S. Cheng, R.E. Amaro, D. Xu, W.W. Li, P.W. Arzberger, J.A. McCammon, Ensemble-based virtual screening reveals potential novel antiviral compounds for avian influenza neuraminidase, J. Med. Chem. 51 (2008) 3878–3894.
[33] M.O. Sinnokrot, E.F. Valeev, C.D. Sherrill, Estimate of the Ab initio for π-π interactions: the benzene dimer, J. Am. Soc. Chem. 124 (2002) 10887–10893.
[34] J.R. Proudfoot, The evolution of synthetic oral drug properties, Bioorg. Med. Chem. Lett. 15 (2005) 1087–1090.
[35] J.M. Miller, A. Dahan, D. Gupta, S. Varghese, G.L. Amidon, Enabling the intestinal absorption of highly polar antiviral agents: ion-pair facilitated membrane permeation of zanamivir heptyl ester and guanidino oseltamivir, Mol. Pharm. 7 (2010) 1223–1234.
[36] K.-C. Liu, P.-S. Lee, S.-Y. Wang, Y.-S.E. Cheng, J.-M. Fang, C.-H. Wong, Intramolecular ion-pair prodrugs of zanamivir and guanidino-oseltamivir, Bioorg. Med. Chem. 19 (2011) 4796–4802.
[37] A.S. Woods, S. Ferre, Amazing stability of the arginine-phosphate electrostatic interaction, J. Proteome. Res. 4 (2005) 1397–1402.

[38] A. Pantos, I. Tsogas, C.M. Paleos, Guanidinium group: a versatile moiety inducing transport and multicompartmentalization in complementary membranes, Biochim. Biophys. Acta 1778 (2008) 811–823.
[39] J.O. Straub, An environmental risk assessment for oseltamivir (Tamiflu) for sewage works and surface waters under seasonal-influenza- and pandemic-use conditions, Ecotoxicol. Environ. Saf. 72 (2009) 1625.
[40] A.F. Stepan, G.W. Kauffman, C.E. Keefer, P.R. Verhoest, M. Edwards, Evaluating the differences in cycloalkyl ether metabolism using the design parameter "lipophilic metabolism efficiency" (LipMetE) and a matched molecular pairs analysis, J. Med. Chem. 56 (2013) 6985–6990.
[41] G. Jones, P. Willett, R.C. Glen, Molecular recognition of receptor sites using a genetic algorithm with a description of desolvation, J. Mol. Biol. 245 (1995) 43–53.
[42] G. Jones, P. Willett, R.C. Glen, A.R. Leach, R. Taylor, Development and validation of a genetic algorithm for flexible docking, J. Mol. Biol. 267 (1997) 727–748.
[43] W.D. Cornell, P. Cieplak, C.I. Bayly, I.R. Gould, K.M. Merz, D.M. Ferguson, D.C. Spellmeyer, T. Fox, J.W. Caldwell, P.A. Kollman, A second generation force field for the simulation of proteins, nucleic acids, and organic molecules, J. Am. Chem. Soc. 117 (1995) 5179–5197.
[44] J. Gasteiger, M. Marsili, Iterative partial equalization of orbital electronegativity – a rapid access to atomic charges, Tetrahedron 36 (1980) 3219–3228.
[45] Y. Watanabe, S.-i. Maehara, Some properties of cyclic phosphoramidites and their phosphites: phosphitylation, ester exchange, and hydrolysis, Heterocycles 52 (2000) 799–810.
[46] L.J. Reed, H. Müench, A simple method of estimating fifty percent endpoints, Am. J. Hyg. 27 (1938) 493–497.
[47] F.G. Burleson, T.M. Chambers, D.L. Wiedbrauk, Virology, a Laboratory Manual, Academic Press, San Diego, CA, USA, 1992.